Technical Report 113
High-Temperature Dielectric Measurements on Radome Ceramics in the Microwave Region

Technical Report 114
A 50-kMc Dielectrometer

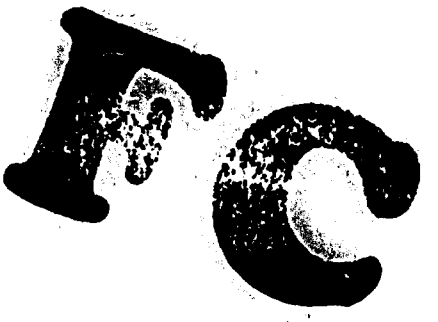

Technical Reports 113 and 114
Laboratory for Insulation Research
Massachusetts Institute of Technology

January, 1957

Technical Report 113

High-Temperature Dielectric Measurements on Radome Ceramics in the Microwave Region

by

W. B. Westphal

Laboratory for Insulation Research
Massachusetts Institute of Technology
Cambridge, Massachusetts

Contract Nonr-1841(10)

January, 1957

HIGH-TEMPERATURE DIELECTRIC MEASUREMENTS ON RADOME CERAMICS IN THE MICROWAVE REGION

by

W. B. Westphal

Laboratory for Insulation Research
Massachusetts Institute of Technology
Cambridge, Massachusetts

Abstract: The dielectric constant and loss of certain ceramics have been measured up to peak temperatures ranging from 500° to 1200°C with a view of the possible use of some of them as radome materials. Their characteristics are compared with those of certain glasses and crystals. Two main types of loss appear: conduction loss increasing exponentially with temperature, and absorptions centered in the infrared which prove to be nearly temperature-independent at microwave frequencies at temperatures below the softening range. Both losses depend on chemical purity, but quantitative interrelation has not been established. A high-purity alumina ceramic having $\kappa' = 9.32$ and $\tan \delta = 0.00015$ at 25°C with changes to 10.4 and 0.0011 at 1200°C and 50 kMc proved to be outstanding as a low-loss material. Some special techniques using the standing wave method in shorted waveguides are discussed briefly.

The electrical properties desired for most high-temperature radomes are moderately low loss ($\tan \delta < 0.01$) and a dielectric constant which decreases slightly with temperature in order to maintain constant electrical wall thickness. Since the wall thickness is often a half wave length, the dielectric constant should be low for higher frequencies.

The materials that might satisfy the electrical requirements are mostly inorganic oxides, and their number is not large (BeO, diamond, MgO, Al_2O_3, SiO_2, CaO, $MgSiO_3$, ZrO_2 are some examples).

Measurement Procedure

All measurements in the microwave region were made with the standing-wave method in shorted lines.[1] Typical sample sizes for various frequency ranges are given in Tables 1 and 2. The main features of a heated sample holder (Fig. 1) are a water-cooled junction to the standing-wave indicator, a thin-walled neck for thermal isolation, and the heated line section containing the sample. Holders for use up to 550°C were made of fine silver with a silver soldered short; solid silver can serve to 850°C. At higher temperatures a holder bored from platinum rod was used.

Each holder is calibrated in node shift vs. temperature. Accurate measurements involve knowledge of the thermal expansion of sample and holder materials so that corrections for sample clearance and change in cutoff wavelength can be made. These two corrections tend to cancel each other and were not required for the measurement data shown here. The resulting error limit in dielectric constant measurements is approximately 2% at 500°, 3% at 800° and 5% at 1200°C for the materials shown.

Work is in progress to make accurate measurements of the temperature coefficient of κ' on fused SiO_2 and ceramic Al_2O_3. The accuracy of loss measurements varies with frequency and temperature from 5 percent or 0.00003 (whichever is larger) at room temperature and 8600 Mc, to 30% or 0.0003 at 1200°C and 50,000 Mc.

---

1) Cf. W.B. Westphal, "Permittivity in Distributed Circuits" in "Dielectric Materials and Applications," A.R. von Hippel, Ed., Wiley and Sons, New York, 1954, p. 63.

Table 1. Frequency and temperature ranges.

Sample No.		Sample No.	
1	10^2 to 10^7 cycles to 500°C	4	8.6×10^9 cycles to 500°C
1	10^8 " room temperature only	5	1.4×10^{10} " to 800°C
2	3×10^8 " limit not yet established	6	2.4×10^{10} " to 800°C
3	1×10^9 " to 500°C	7	5×10^{10} " to 1200°C
3	3×10^9 " to 500°C	8	d-c resistivity, 1200°C

Table 2. Preferred samples for low-loss materials.

Sample No.	Shape	Diameter in inches	Thickness or length in inches for $\kappa'=4$	$\kappa'=6$	$\kappa'=8$	$\kappa'=10$
1	Disk	1.5 to 2.00 (faces plane, parallel to 0.002 in.)	Thickness 20% tolerance 0.12	0.18	0.24	0.30
2	Disk	1.0±0.1	Thickness 20% tolerance 0.08	0.12	0.15	0.18
3	Coaxial tube (may consist of stacked washers)	o.d. 0.999±0.001 i.d. 0.376±0.001	Length 10% tolerance 1.48	1.20	1.04	0.93
4	Cylinder	0.999±0.001	Length 5% tolerance 1.00	0.77	0.64	0.56
5	Cylinder	0.624±0.0005	Length 5% tolerance 0.574	0.455	0.39	0.344
6	Cylinder	0.374 ±0.0005	Length 5% tolerance 0.35	0.277	0.236	0.21
7	Cylinder	0.1712±0.0003	Length 5% tolerance 0.164	0.133	0.113	0.100
8	Rod, round or square	1/8 to 3/8 in.	Length 1 ± 1/8 in.	independent of κ'		

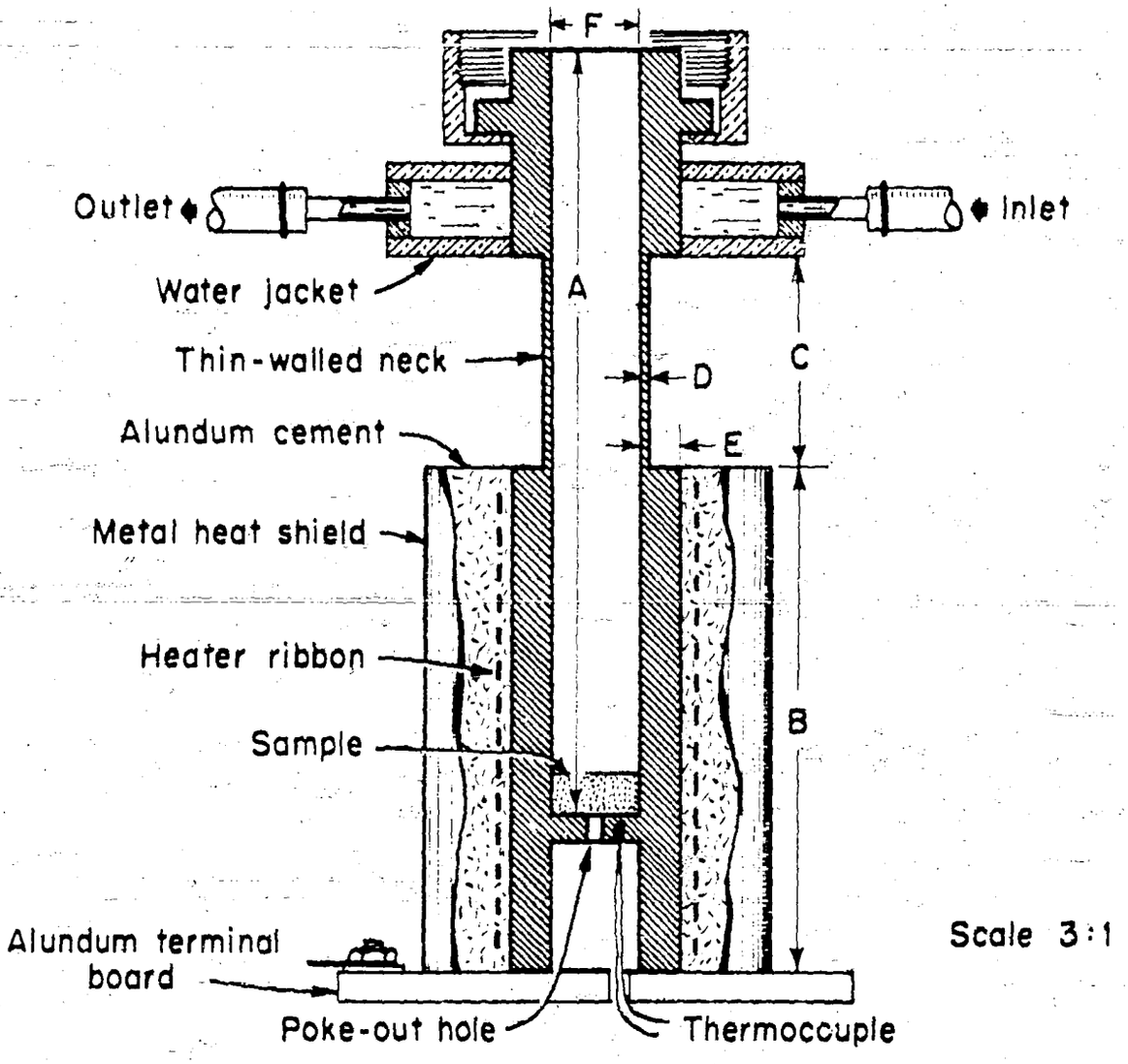

Fig. I. Longitudinal section of circular, high-temperature sample holders. Typical dimensions are as follows:

	Nominal frequency	8.6×10^9	1.4×10^{10}	2.4×10^{10}	5×10^{10}
A.	Inside length	15.0 cm	7 cm	5.3 cm	3.1 cm
B.	Length heated	10.0 cm	4.2 cm	3.6 cm	2.4 cm
C.	Length of neck	3.6 cm	2.1 cm	1.0 cm	0.8 cm
D.	Neck thickness	0.030 in.	0.012 in.	0.010 in.	0.008 in.
E.	Wall thickness	1/8 in.	1/8 in.	1/16 in.	1/16 in.
F.	Inside diameter	1.0 in.	5/8 in.	3/8 in.	11/64 in.

Materials Investigated

Beryllium oxide is not promising because it hydrolyzes at high temperature in the presence of water vapor to poisonous $Be(OH)_2$. Figure 2 taken on a porous ceramic body shows the low dielectric constant (4.4) and moderate loss tangent. Complete drying reduces the loss to less than 0.0005 over the entire frequency range.

Diamond with its strong covalent bonding may be ideal electrically over a wide temperature range. Unfortunately, the measurements[2] made are very limited ($\kappa' = 5.68$, $\frac{d\kappa'}{dT} = +1 \times 10^{-5}$ per $^{\circ}C$).

Both magnesium oxide and calcium oxide have low temperature forms which readily hydrolyze. The periclase (high temperature) phase of MgO

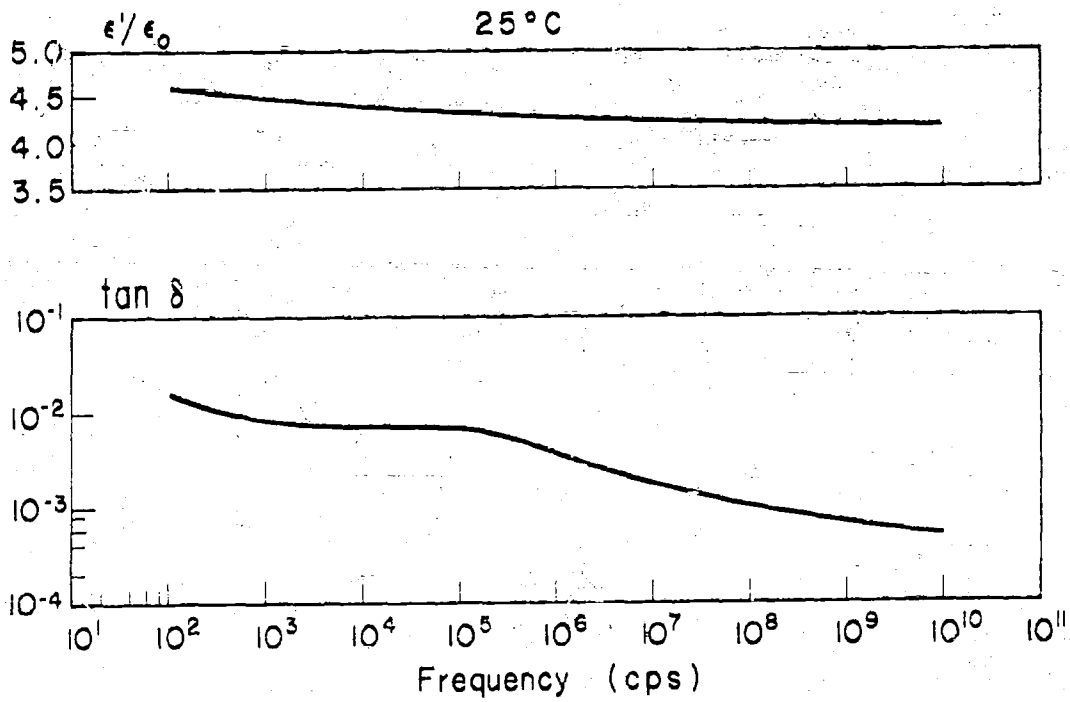

Fig. 2. Dielectric constant and loss tangent vs. frequency for beryllium oxide ceramic (Norton Co.) at room temperature.

---

2) S. Whitehead and W. Hackett, Proc. Phys. Soc. (London) 51, 173 (1939); P. T. Narasimhan, ibid. 68B, 315 (1955).

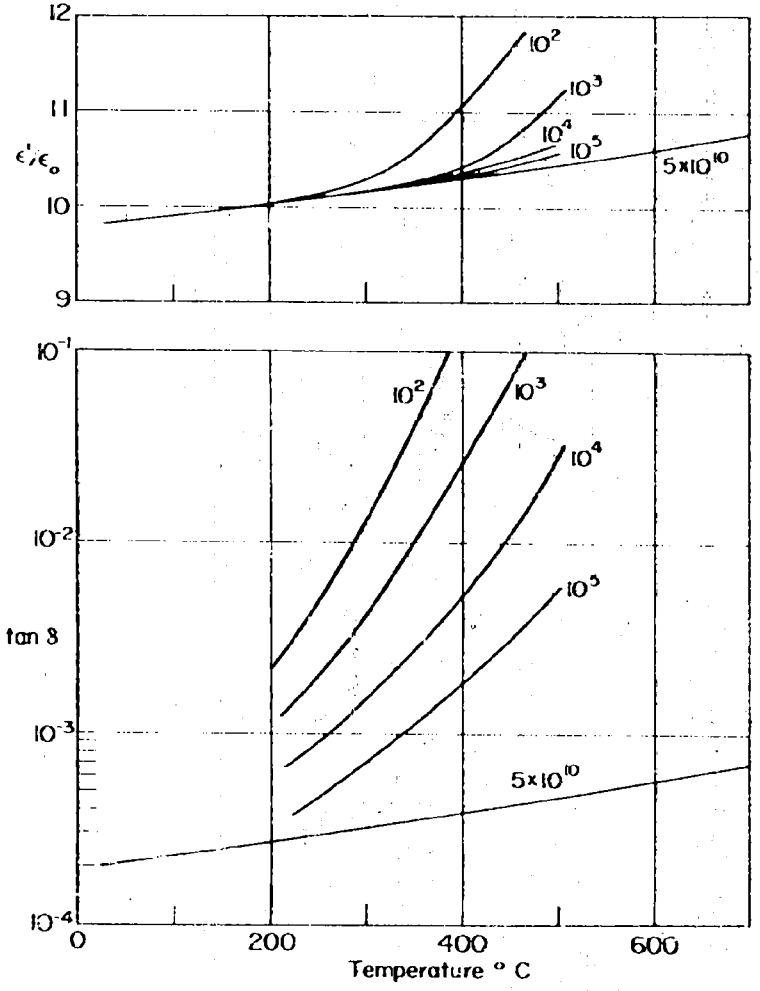

Fig. 3. Dielectric constant and loss tangent vs. temperature of MgO crystal (Norton Co.) at various fixed frequencies.

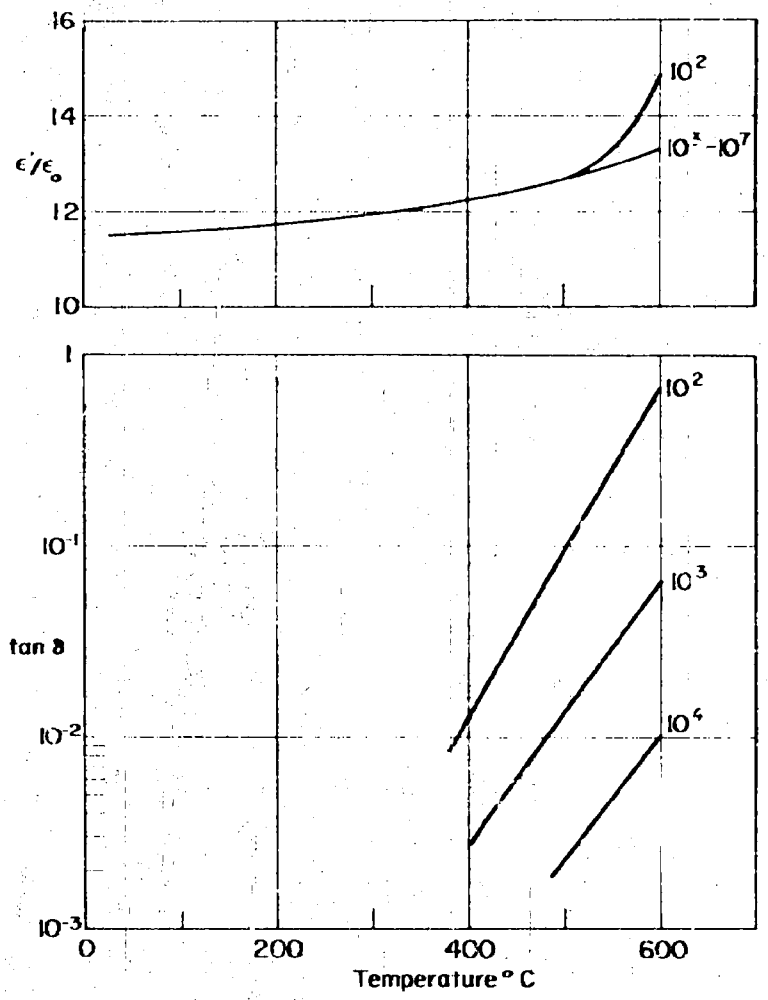

Fig. 4. Dielectric constant and loss tangent vs. temperature of Al_2O_3 crystal (Linde Air Products Co.) at various fixed frequencies. The electric field is parallel to the optic axis; this is the direction of highest conductivity.

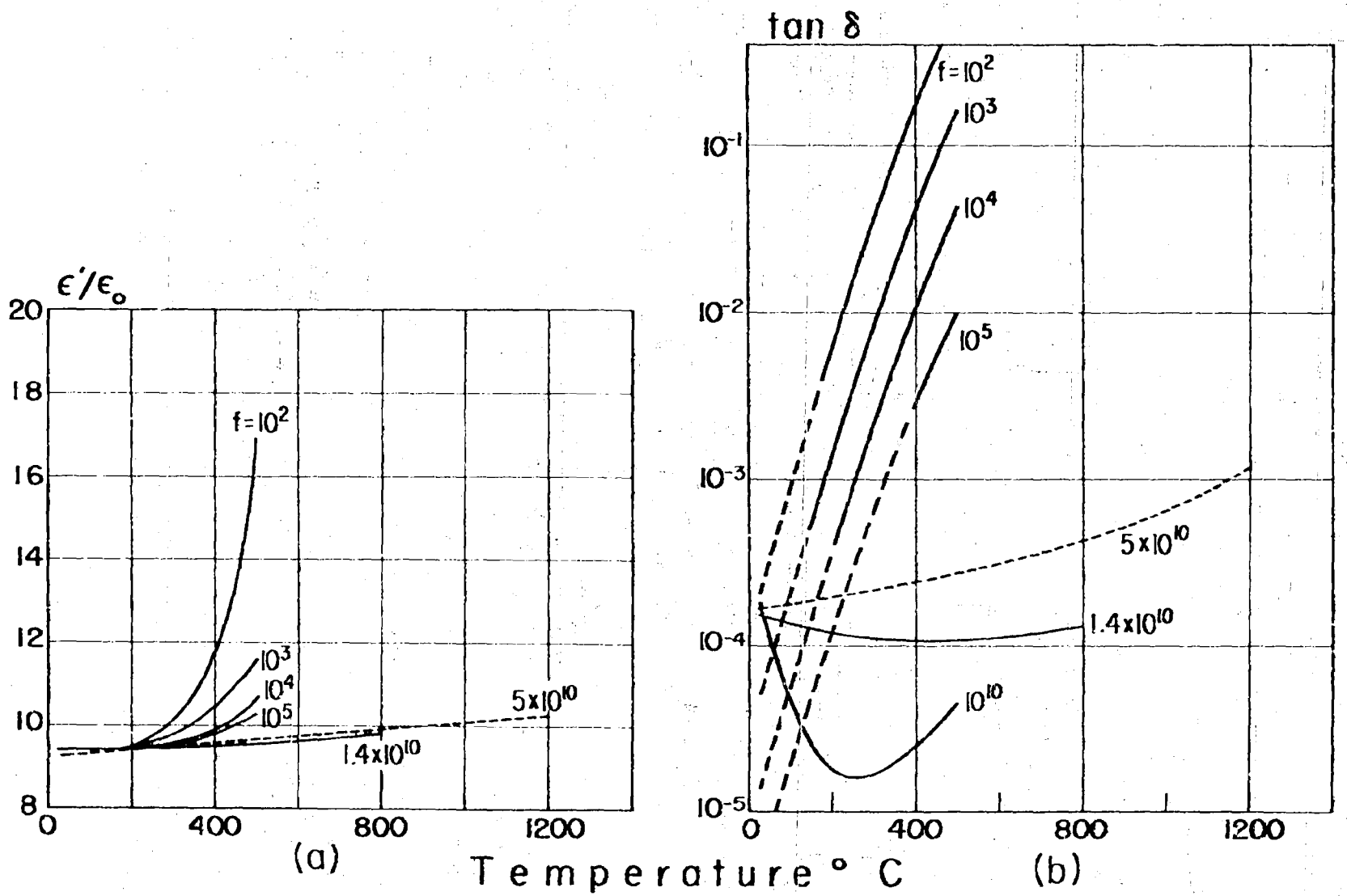

Fig. 5. (a) Dielectric constant and (b) loss tangent vs. temperature of high-purity alumina ceramic (Kearfott Co.) at various fixed frequencies.

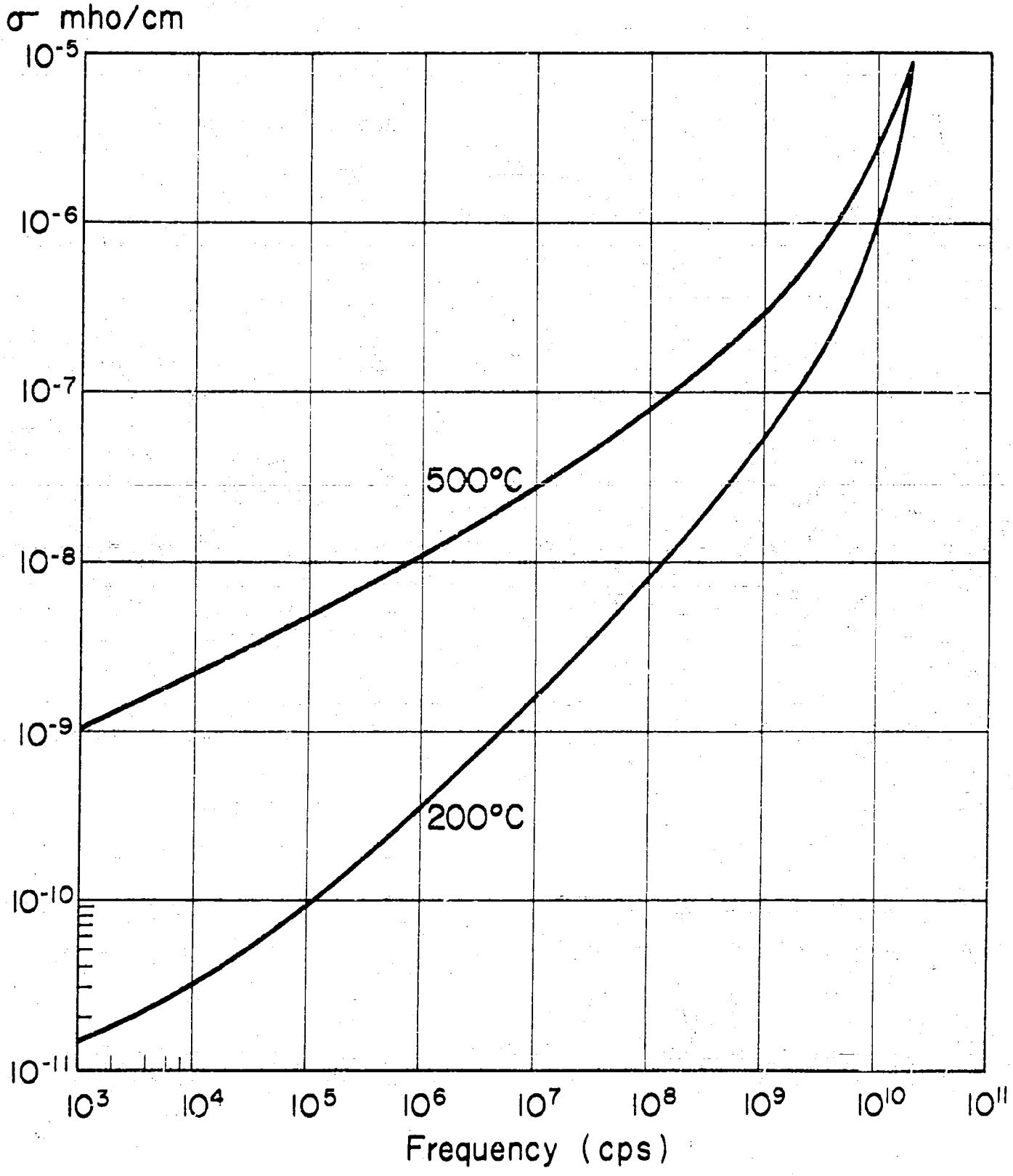

Fig. 6. Volume conductivity vs. frequency of high-purity alumina ceramic (Kearfott Co.) for two temperatures.

should be excellent. In Fig. 3 the dielectric constant and loss of a synthetic single crystal is shown. The conductivity (calculated at 100 cps from $\sigma = \omega \epsilon_o \frac{\epsilon'}{\epsilon_o} \tan \delta$ is much lower than values reported in the literature.[3)]

Synthetic white sapphire (Al_2O_3) has dielectric constants of 9.53 and 11.53 measured $\perp$ and $\parallel$ to the optic axis, respectively. Figure 4 shows high-temperature data on a crystal. Alumina ceramics are common; dielectric constant and loss on a high-purity material are shown in Fig. 5. The volume conductivity plotted for two different temperatures (Fig. 6) serves to emphasize the fact that the microwave loss is not due to conduction, as it is in the low frequency range. The decreasing loss tangent with temperature at 10^{10} cycles may be due to moisture loss.

Data on a commercial high alumina body (Fig. 7) show that the low frequency loss at high temperatures is about 50 times larger and the 10,000 Mc loss about 20 times larger than for the high-purity material. The chemical analysis indicates that ionized $Ca(OH)_2$ that may be present is responsible for its higher loss; perhaps also the firing temperature in the manufacture was too low and some of the MgO is not in the periclase form. Figure 8 shows data on a commercial alumina-mullite ($3\ Al_2O_3 \cdot 2\ SiO_2$). Data on about 30 other alumina bodies will be given in the forthcoming Tables of Dielectric Materials, volume V.

Fused silica[4)] has a low dielectric constant (3.78) and temperature coefficient (3×10^{-5}); dielectric constant and loss have been measured on material from two sources (Figs. 9 and 10).

It is well known that the addition of impurity ions causes large increases in the low-frequency conductivity, especially for small ions which can move

---

3) A. Lempicki, Proc. Phys. Soc. (London) 66B, 281 (1953); E. Yamaka and K. Sawamoto, Phys. Rev. 95, 848 (1954).

4) J.P. Pérez, Ann. phys. [12] 7, 238 (1952).

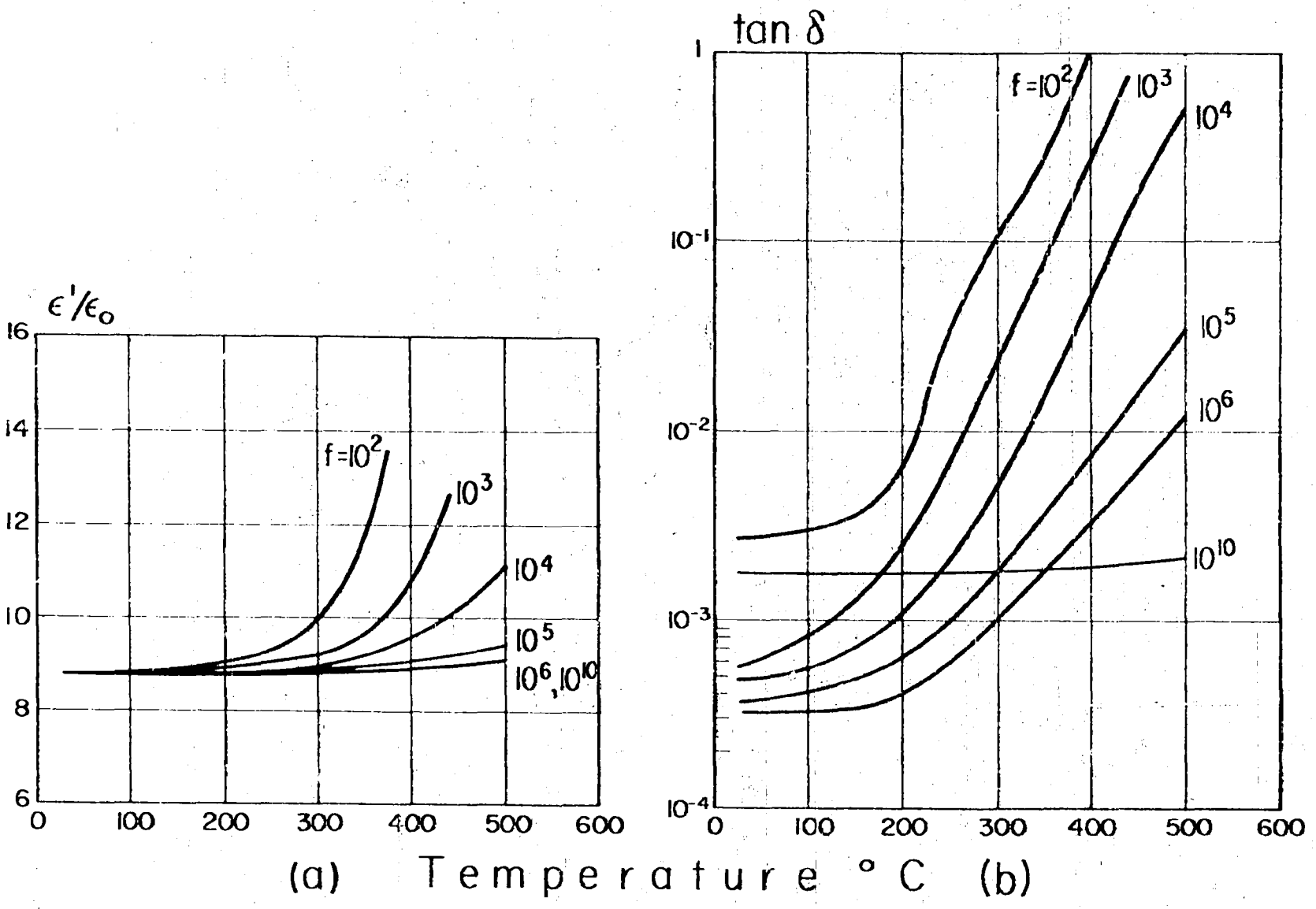

Fig. 7. (a) Dielectric constant and (b) loss tangent vs. temperature of high alumina body (95.78% Al_2O_3, 2.96% SiO_2, 1.12% CaO, 0.16% MgO; No. AI-200, Coors Porcelain Co.) at various frequencies.

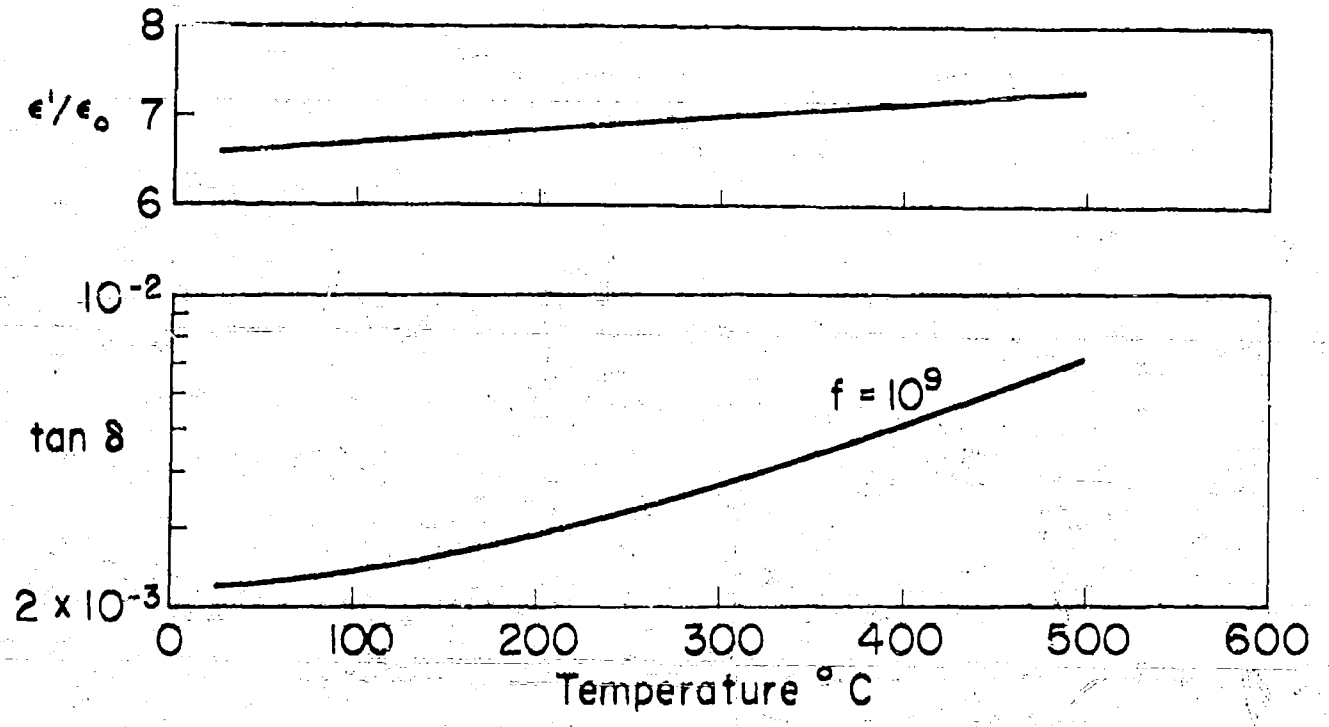

Fig. 8. Dielectric constant and loss tangent of alumina-mullite body (No. 7873, Frenchtown Porcelain Co.) at 10^9 cps.

easily through the silicon-oxygen network.[5] The microwave loss may be caused by vibrations of loosely bound alkali ions in their oxygen surroundings. This loss is practically not changed with temperature until the softening region is reached. Microwave data on a group of silica glasses (Fig. 11) indicate that this loss progressively increases from a lithium to a sodium to a potassium glass as one would expect when the vibration frequency moves with increasing mass of the cation to lower frequency. Rubidium oxide does not form a stable glass phase and shows a lower loss.

As has been previously stated, CaO reacts with moisture readily and no commercial ceramics are made of this oxide. Scandium oxide and vanadium oxide are probably not as thermally stable as MgO or Al_2O_3, but offer promise of usefulness. No data are available. Titanium dioxide in

5) Cf. J.M. Stevels, Philips Tech. Rev. 13, 360 (1952).

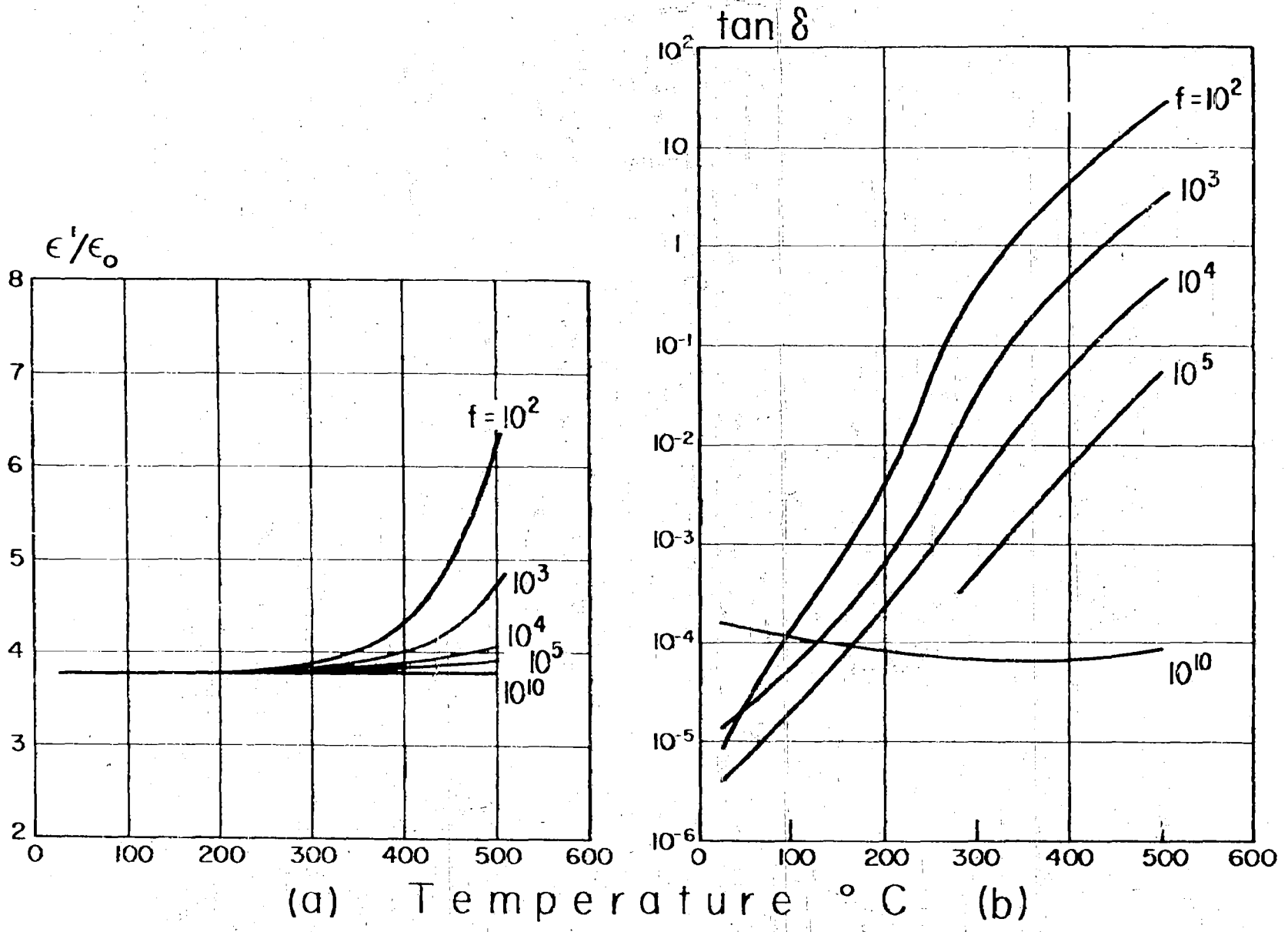

Fig. 9. (a) Dielectric constant and (b) loss tangent vs. temperature of fused silica (No. 915 C, Corning Glass Works) at various fixed frequencies.

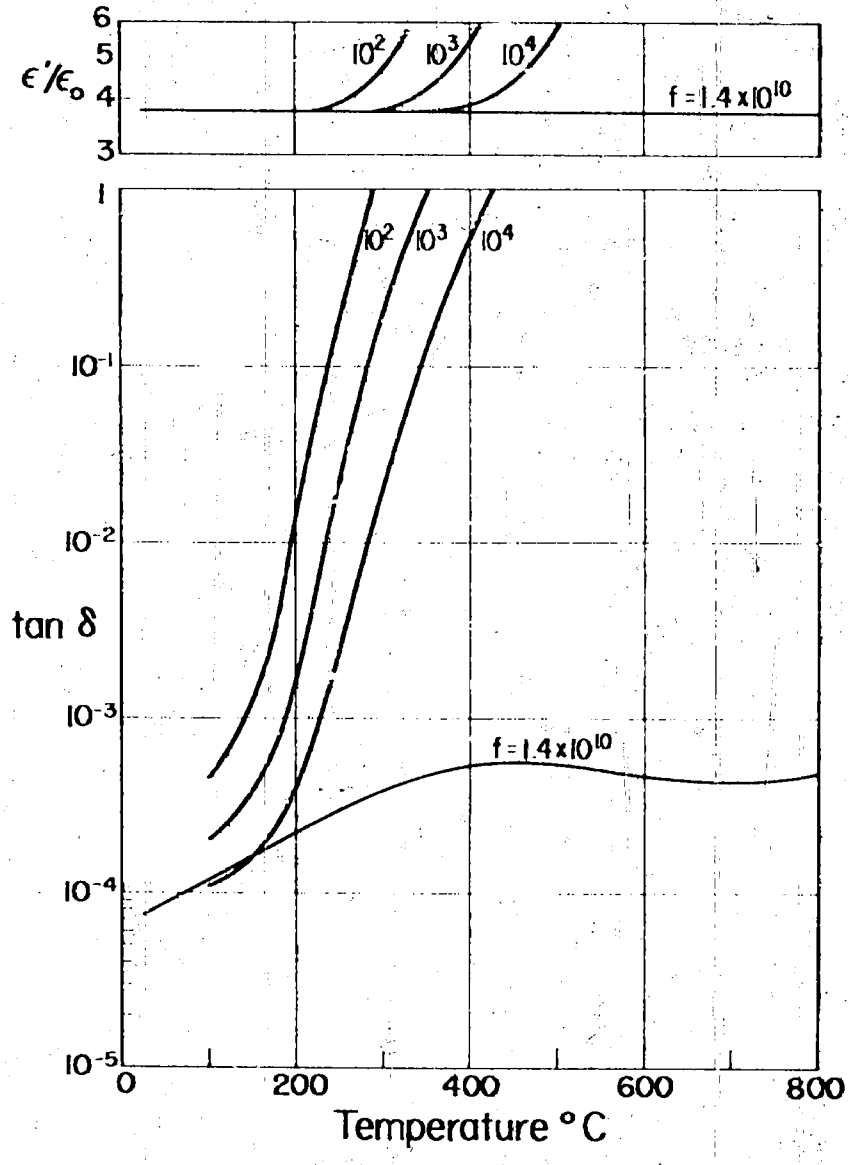

Fig. 10. Dielectric constant and loss tangent vs. temperature of fused quartz (General Electric Lamp Works) at various fixed frequencies.

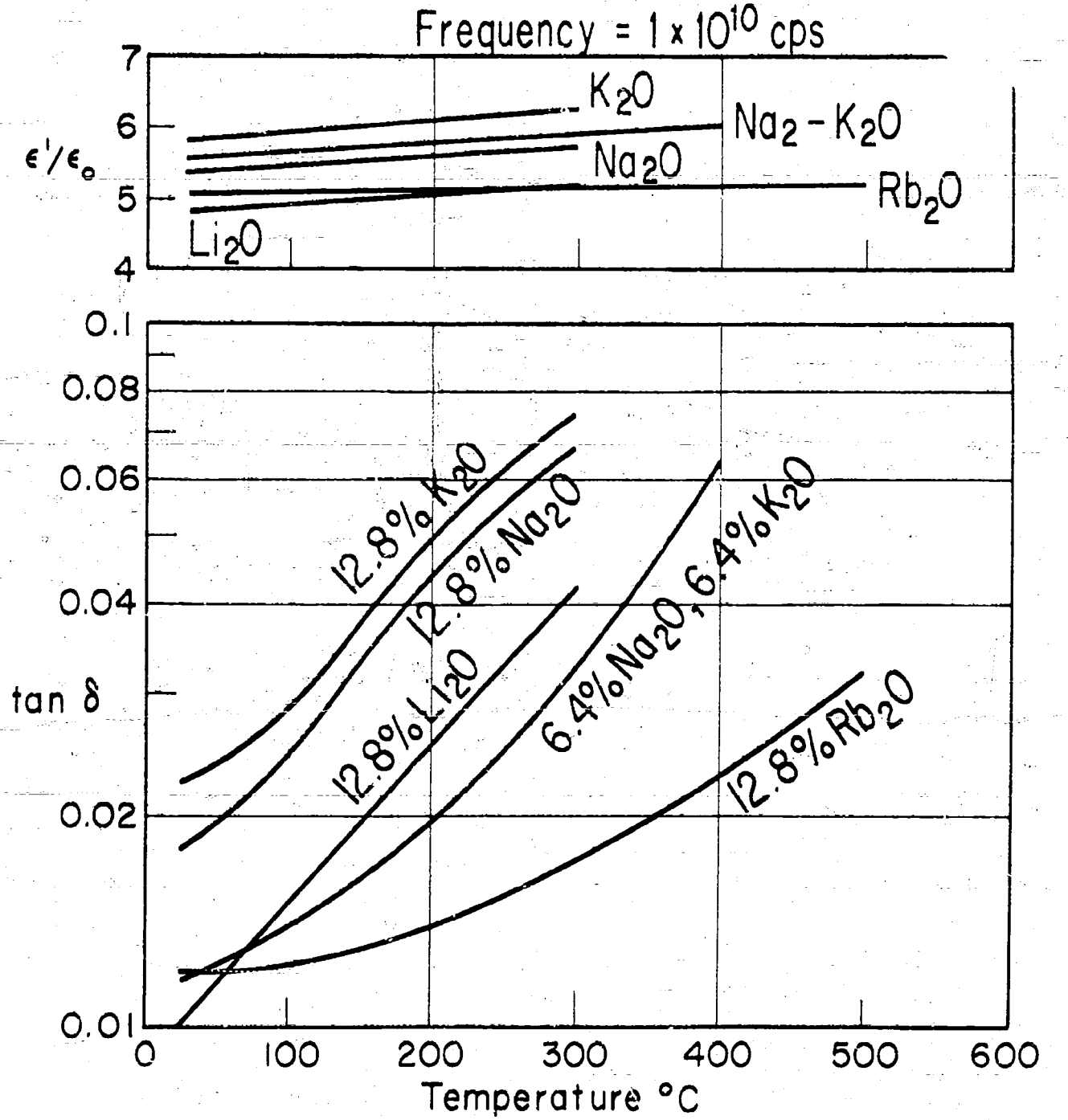

Fig. 11. Dielectric constant and loss tangent vs. temperature of a group of alkali-silica glasses (Lab. Ins. Res.) at 10^{10} cps.

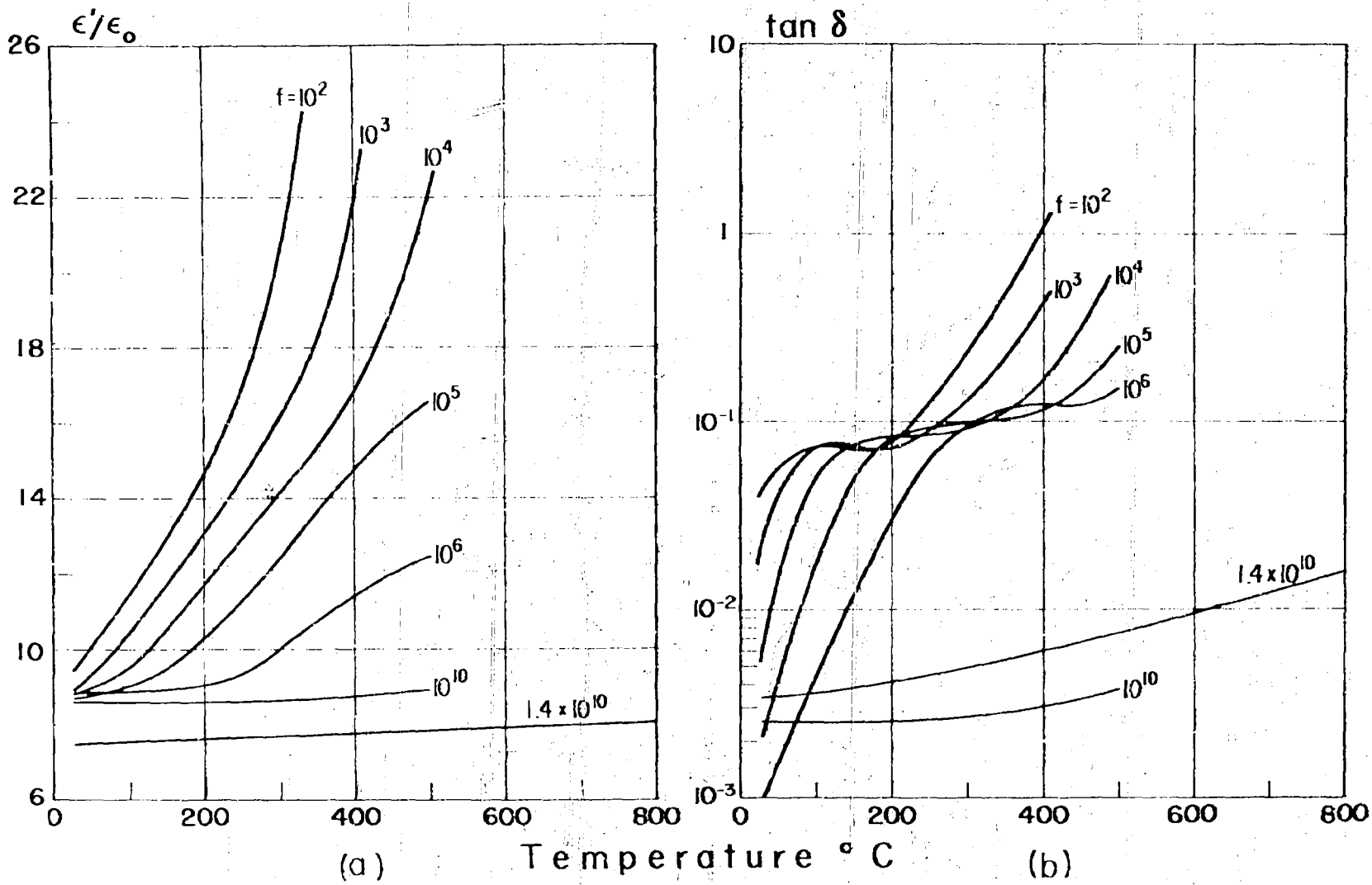

Fig. 12. (a) Dielectric constant and (b) loss tangent vs. temperature of zircon porcelain (AlsiMag 477, American Lava Corp.) at various fixed frequencies. The density of the samples used in the range 10^2 to 10^{10} cps was 3.69 g/cm^2, and that used at 1.4×10^{10} cps was 3.43 g/cm^2.

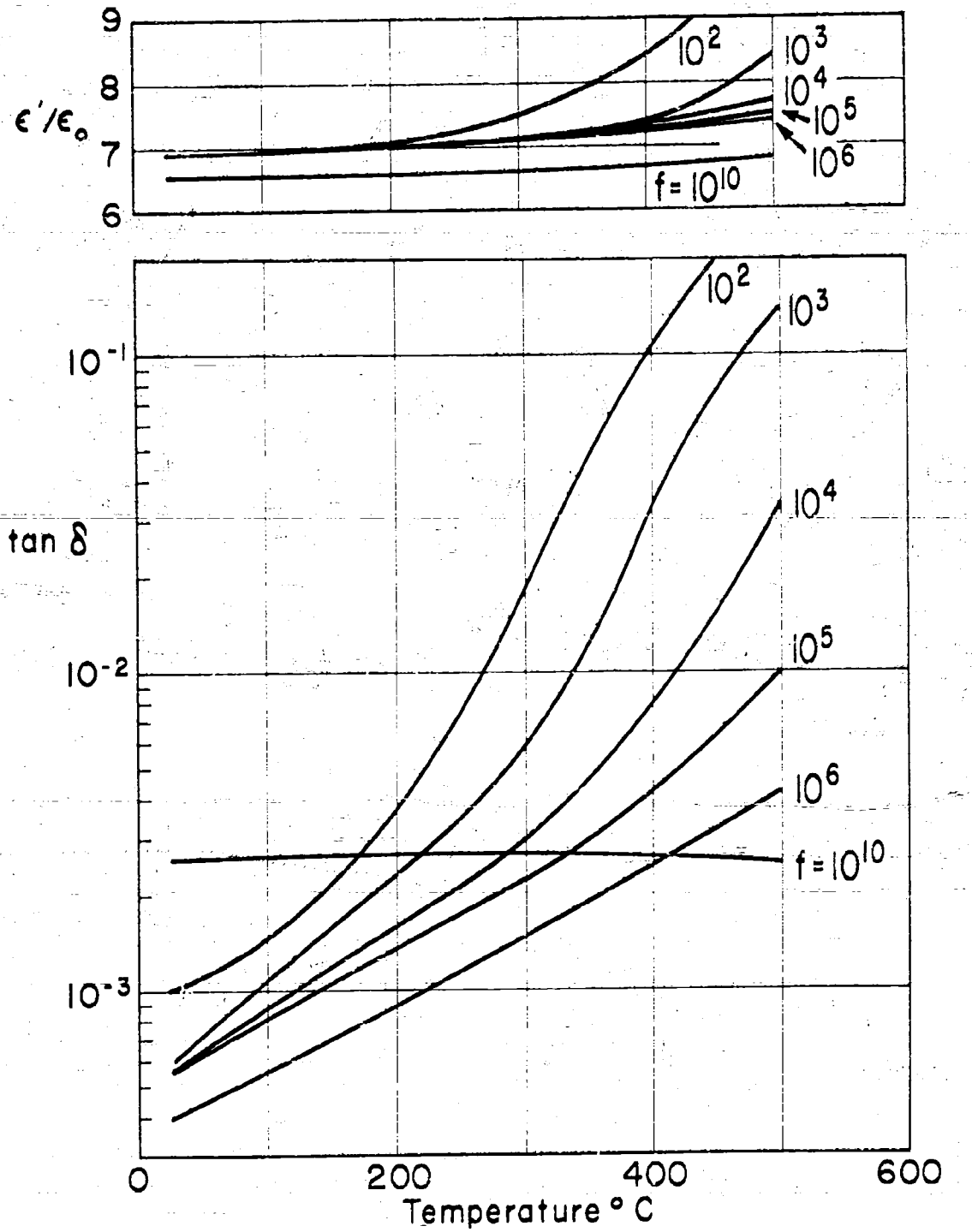

Fig. 13. Dielectric constant and loss tangent vs. temperature of wollastonite body (AlsiMag 577, American Lava Co.) at various fixed frequencies.

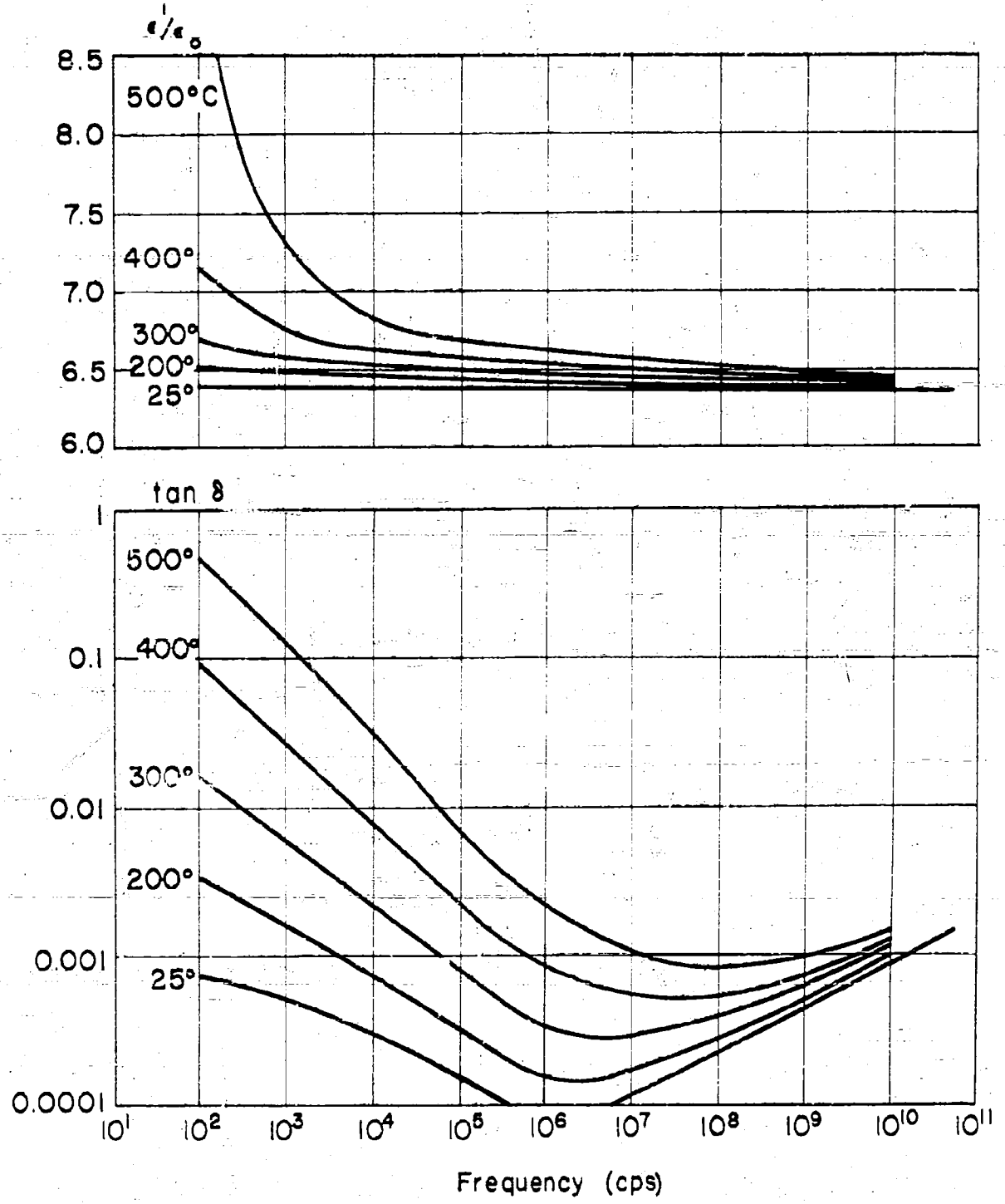

Fig. 14. Dielectric constant and loss tangent vs. frequency for a low loss steatite (F-66, 60% talc, 15% kaolin, 17.5% $BaCO_3$, 7.5% $MgCO_3$, Bell Telephone Labs.) at various temperatures.

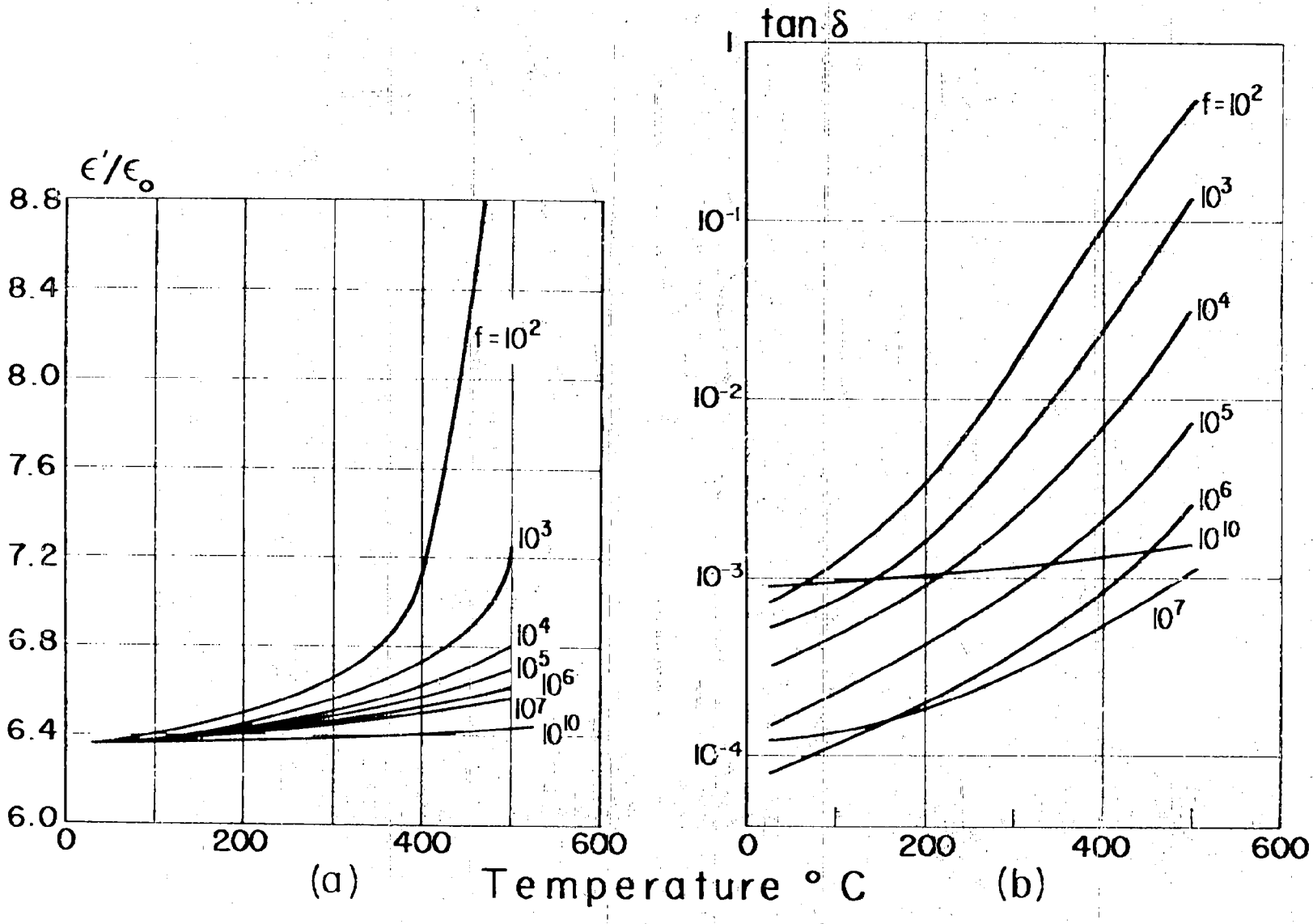

Fig. 15. (a) Dielectric constant and (b) loss tangent vs. temperature for the steatite of Fig. 14 at various fixed frequencies.

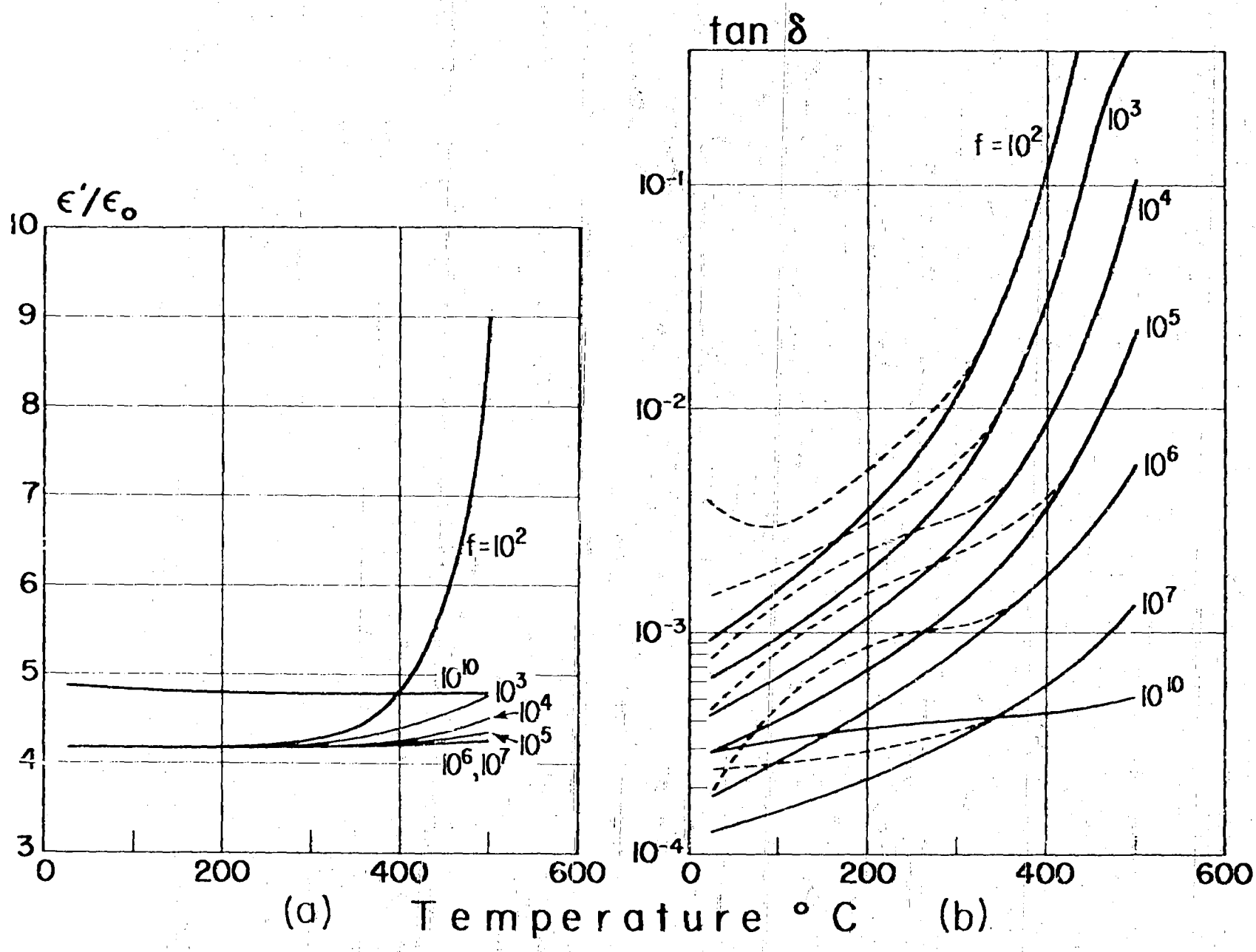

Fig. 16. (a) Dielectric constant and (b) loss tangent vs. temperature of hot-pressed boron nitride (Carborundum Co.) at various fixed frequencies. Data at 10^{10} cycles were taken with electric field $\perp$ to direction of pressing; at other frequencies field is $\parallel$.

rutile form has a high dielectric constant (ca. 100) and tends to reduce easily to a highly conductive form.[6] Its negative temperature coefficient is useful in mixes with other oxides.

Commercial zirconium oxide bodies vary over a wide range. Figure 12 gives the data for one of the lowest loss materials.

Calcium silicate (wollastonite) in commercial quality is shown in Fig. 13.

Magnesium silicate is one of the main ingredients in commercial steatite bodies. The dielectric constant and loss vs. frequency (Fig. 14) and vs. temperature (Fig. 15) are given for one of the best grades of this material.

Boron nitride has excellent electrical properties in the dry state (solid lines, Fig. 16). This material apparently reacts with water at high temperatures. The samples are not isotropic since the direction of crystal growth is influenced by high forming pressure.

An alloy of boron nitride and silicon nitride proved to have fairly high loss and the dielectric constant was decreased after the temperature run, as indicated in Fig. 17.

A sample of one of the newer glass-mica combinations was cut from a circular rod for measuring as a function of temperature (Fig. 18). The sample cross section became increasingly elliptic, hence measurements were not made above ca. 400°C.

Conclusions

The electrical performance of all materials tested would be satisfactory for radome use up to our highest measuring temperature. High-purity alumina bodies offer the possiblity of satisfactory operation above

6) A. von Hippel et al., Report No. 540, Oct., 1945, N.D.R.C. Div. 14, Contract OEMsv-191, Lab. Ins. Res., Mass. Inst. Tech.

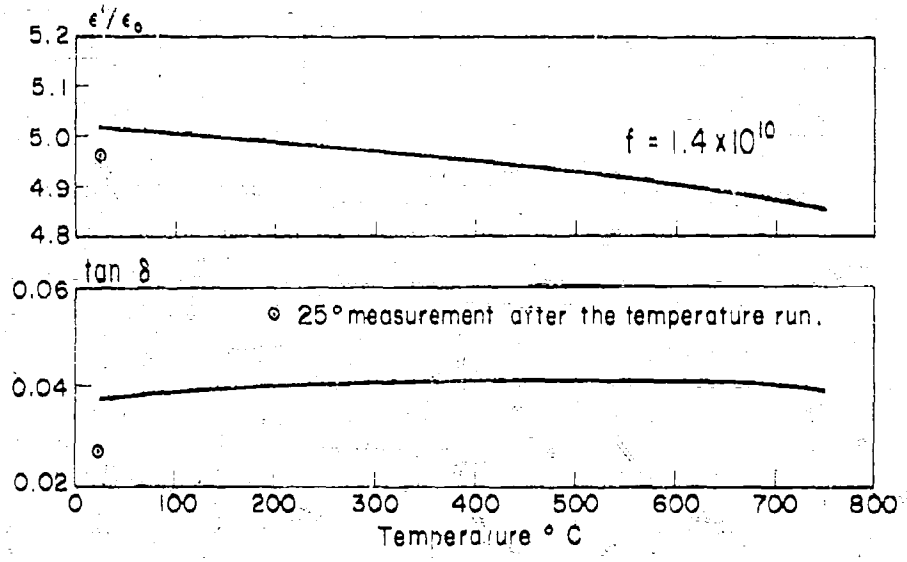

Fig. 17. Dielectric constant and loss tangent vs. temperature of an alloy of silicon nitride (75%) and boron nitride (25%) (Carborundum Co.) at 14, 000 Mc.

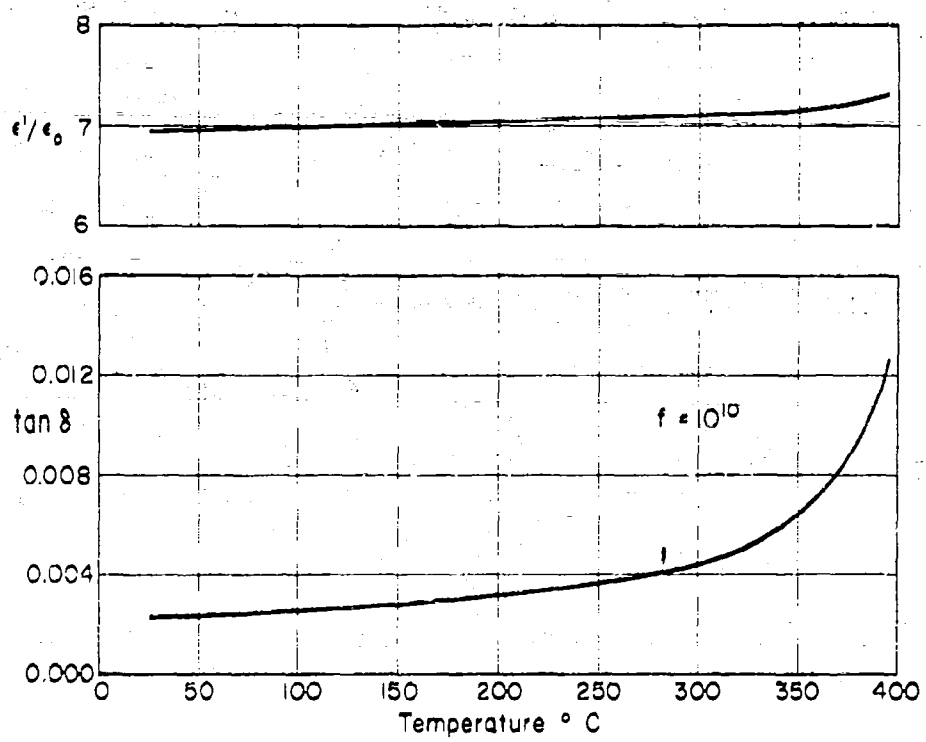

Fig. 18. Dielectric constant and loss tangent vs. temperature for synthetic mica bonded with glass (Supramica 500, Mycalex Corp.) at 10, 000 Mc.

1200°C. The need for a further extension of our measurement range to still higher temperatures is indicated.

Acknowledgements

Especial thanks are due to Professors A.R. von Hippel and G. Economos for their helpful discussions. Many of the measurements and calculations were made by Mrs. B.B. East.

Technical Report 114

A 50-kMc Dielectrometer

by

N. E. Dye

Laboratory for Insulation Research
Massachusetts Institute of Technology
Cambridge, Massachusetts

Contract Nonr-1841(10)

January, 1957

A 50-kMc DIELECTROMETER

by

N. E. Dye

Laboratory for Insulation Research
Massachusetts Institute of Technology
Cambridge, Massachusetts

Abstract: A dielectrometer, using the standing-wave method with circular wave guide, has been developed which permits measurements of the complex permittivity and permeability of materials at 50 kMc. The instrument is capable of measuring relative dielectric constants from 1 to 100 and loss tangents as low as 0.0001. Only small samples are required and measurements can be made over a wide temperature range up to 1200°C.

Special developmental problems concerning the crystal detector, slotted section, and probe are discussed in detail. Typical dielectric measurements on various samples are appended.

Introduction

The basic theory of the standing-wave method for measuring dielectric properties of materials, as developed by the Laboratory for Insulation Reserach,[1] is well known, and its application in the microwave range of the frequency spectrum has been described in detail.[2]

When a sample is placed in a shorted section of wave guide, the nodes of the standing-wave pattern are shifted and broadened. Measurement of these changes allows calculation of the relative dielectric constant κ' and the loss

1) S. Roberts and A. von Hippel, J. Appl. Phys. 17, 610 (1946).

2) W. B. Westphal in "Dielectric Materials and Applications," A. R. von Hippel, Ed., Wiley and Sons, New York, 1954, pp. 63-122.

tangent, tan δ, of the material, provided the guide wave length λ_g, cutoff wave length λ_c and length of sample d are known. The basic equations are

$$\kappa' \equiv \frac{\epsilon'}{\epsilon_o} = \frac{\left(\frac{\lambda_g}{\lambda_c}\right)^2 + \left[\frac{\lambda_g}{2\pi d}\,(\beta_2 d)\right]^2}{1 + \left(\frac{\lambda_g}{\lambda_c}\right)^2} \qquad (1)$$

where the phase constant β_2 of the sample is found by graphical solution of the transcendental equation

$$\frac{\tan \beta_2 d}{\beta_2 d} = -\frac{\lambda_g}{2\pi d} \tan \frac{2\pi x_o}{\lambda_g} \qquad (2)$$

with x_o the distance from sample surface to the first minimum.

The loss tangent is calculated as:

$$\tan \delta = \frac{\Delta x}{d} \cdot \frac{\beta_2 d \left[1 + \tan^2 \frac{2\pi x_o}{\lambda_g}\right]}{\beta_2 d \left(1 + \tan^2 \beta_2 d\right) - \tan \beta_2 d} \cdot \frac{w - u \frac{\epsilon_o}{\epsilon'}}{w} \qquad (3)$$

where Δx is the node width, the distance between points of twice minimum power; $u = \lambda_g^2/\lambda_c^2$ and $w = 1 + u$.

The principal components of a dielectrometer are shown in Fig. 1. Its central feature is the standing-wave indicator (henceforth abbreviated SWI), consisting of a slotted section of wave guide and a traveling detector. The associated equipment (square-wave modulator, tuned amplifier, and necessary power supplies) are conventional in design and will not be discussed further.

Mechanically, the indicator must provide rectilinear motion of the probe along the slot together with precise measurements of this motion to an accuracy of at least 10^{-3} mm. Electrically, the indicator must be so designed that the introduction of slot and probe into the wave guide will produce a negligible

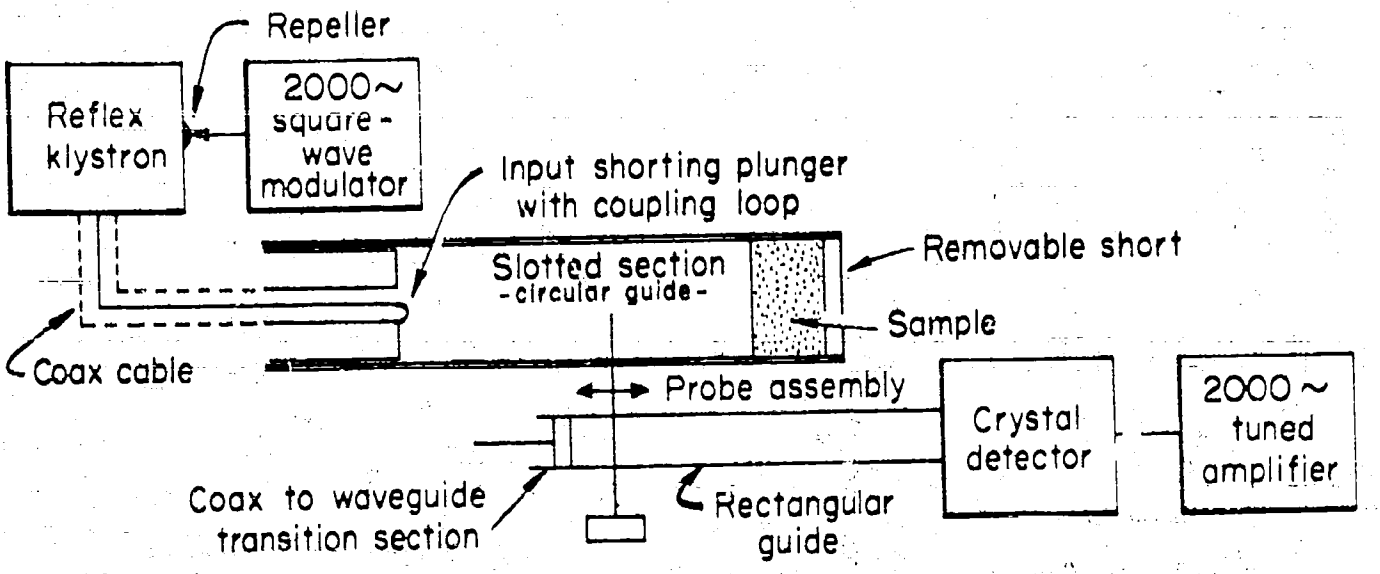

Fig. 1. Typical microwave dielectrometer.

effect on the field pattern.

Other requirements for a satisfactory SWI are: provisions for tuning the wave guide section to resonance, a removable sample holder, an adjustment for probe depth, probe tuning devices, and a detector.

The 50-kMc Standing-Wave Indicator

The standing-wave indicator[3] for use at 50 kMc (Figs. 2, 3a and b) consists of two principal parts, a wave guide block and a probe carriage, both made of copper. In the block is a circular wave guide containing a 6-mil slot slightly longer than one guide wave length. An input plunger with a magnetic coupling loop is placed in one end and a removable sample holder is attached to the other end of the guide. The probe carriage contains a 1.5-mil probe in a probe holder, the probe and holder being insulated from the carriage by Teflon beads. The holder is also part of a coax-to-wave-guide transition

3) N.E. Dye, "A Standing-Wave Indicator for Dielectric Measurements at 50 kMc," S.M. Thesis, E.E Department, Mass. Inst. Tech., 1955.

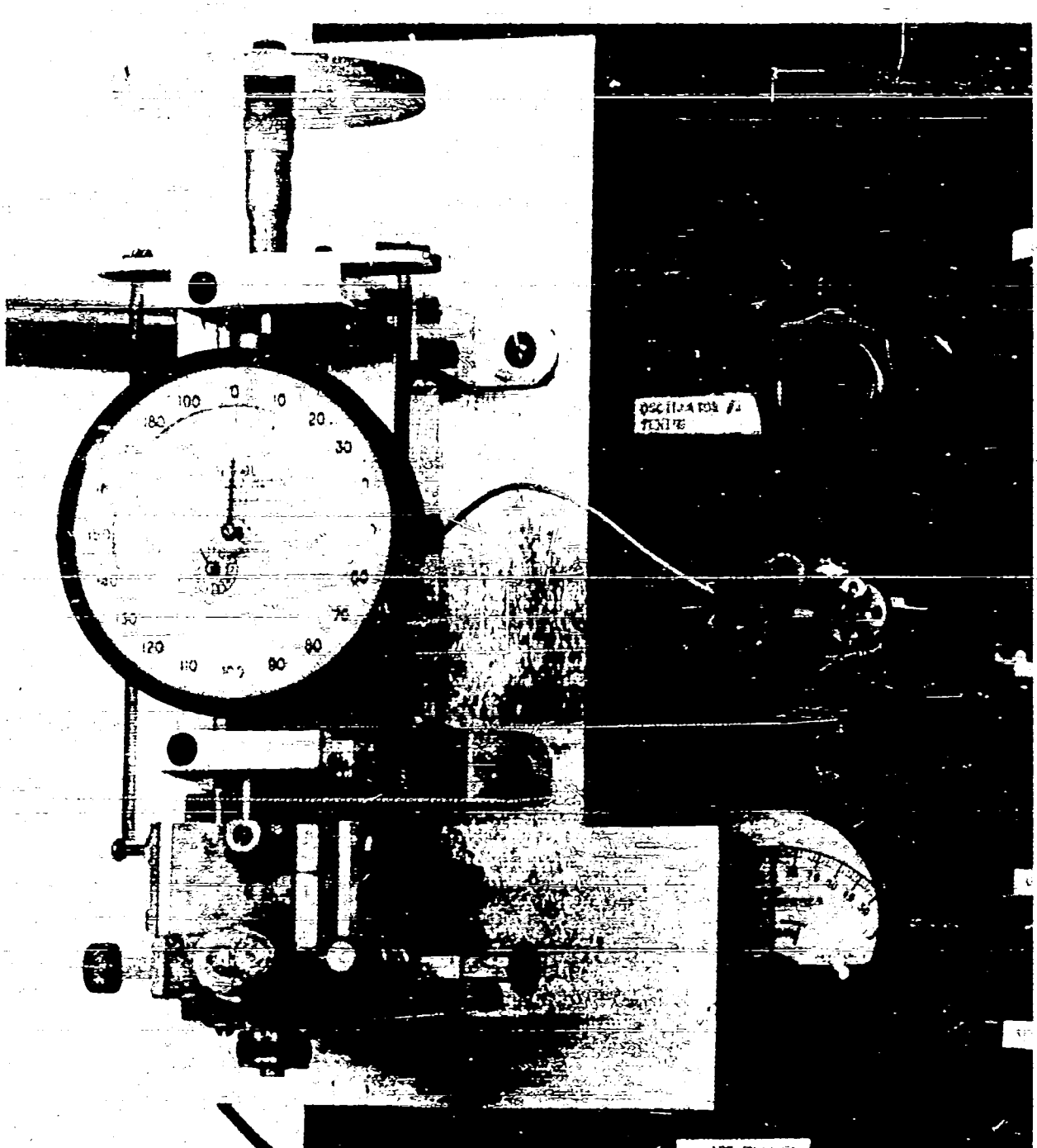

Fig. 2. Standing-wave indicator for 50-kMc dielectrometer.

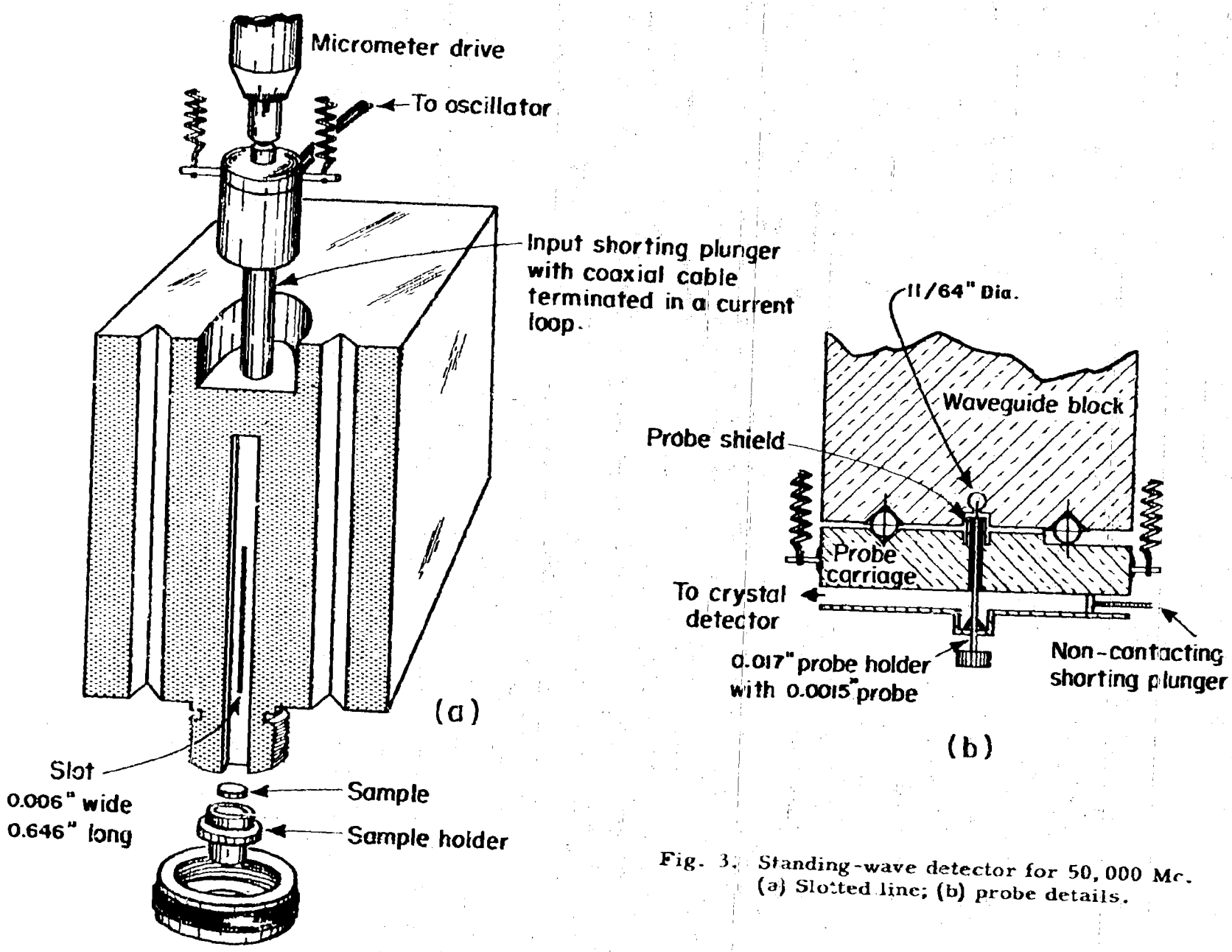

Fig. 3. Standing-wave detector for 50,000 Mc. (a) Slotted line; (b) probe details.

section built into the top of the probe carriage. Signals picked up by the probe travel along the coaxial cable into the rectangular guide, and finally to a crystal detector. Both sample block and probe carriage contain slots that together form a noncontacting probe shield (Fig. 3b).

Essentially the 50-kMc SWI is a scaled-down version of lower frequency models. Its unique features, discussed in the following paragraphs, arise from the adaptation of known principles to higher frequencies.

Frequency Source and Input Plunger

A reflex klystron (Raytheon QK 294) serves as a primary source of the 50-kMc energy. The QK 294 is rated for 5-mw maximum output with average outputs of 3 mw. This output power, available in a rectangular wave guide, is coupled to a miniature coaxial cable (Amphenol RG 174/U or Microdot) by a probe-type transition section. The cable is terminated in a loose-coupled magnetic loop located in the face of a noncontacting circular shorting plunger. It is preferable to use miniature cable with Teflon dielectric and solid center conductor; these features facilitate construction of the loop which is made by bending the center conductor over a small rod, then soldering to a silver sleeve that has been attached to the braided shield. The sleeve is then press-fitted into the face of the shorting plunger. A typical loop is 13 to 20 mils in radius (Fig. 4). The loose coupling, together with the lossy properties of the coaxial cable, eliminates the need for an isolating attenuator in the oscillator output. Such an attenuator is normally required to prevent impedance changes in the SWI from affecting the frequency of the reflex klystron. Accurate positioning of the shorting plunger is achieved by a spring-loaded micrometer.

Pickup Probe

Probes as small as 1 mil in diameter were made with a length of 0.1 in., which permits a maximum probe depth equal to the radius of the guide. In order

to achieve rigidity with such small dimensions, tungsten wire was used. The wire was gold plated to improve its conductivity and to permit soldering into the probe holder (a silver tube 17 mils o.d., 5 mils i.d.).

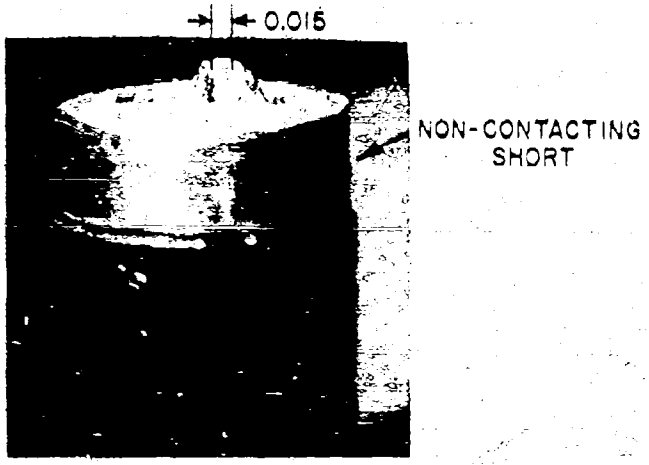

Fig. 4. Enlarged view of input loop.

The best results have been achieved when the tungsten wire was pulled through the silver tube (already placed in the probe carriage) and soldered in place without touching the probe end of the wire. It is difficult to straighten the tungsten once it has been bent; hence, extreme care must be exercised in the soldering process. In general, the probe will stand off center in the silver tube. This is not a serious problem because the probe holder can be rotated until precise lateral centering of the probe in the carriage is achieved. However, it is important that the probe be perpendicular to the axis of the wave guide, i.e., perpendicular to the bottom face of the probe carriage. The probe is approximately 3 times as wide as a typical node in the empty guide. Thus the measurement of node width is really an averaging process, the accuracy of which depends on the straightness and perpendicularity of the probe. (It has not been shown mathematically that node widths can actually be measured using a probe which is wider than the node. However, no adverse effects have been noticed in measurements at 3, 10, and 25 kMc under similar conditions.)

The assembly and adjustment of the probe in the carriage block requires the use of a low power microscope (18 to 100X). A microphotograph of an

actual probe and holder in the carriage block is shown in Fig. 5.

It has been found that the probe-shield choke, shown in Fig. 5, in addition to the main probe shield shown in Fig. 3b, is necessary to reduce radiation from the probe.

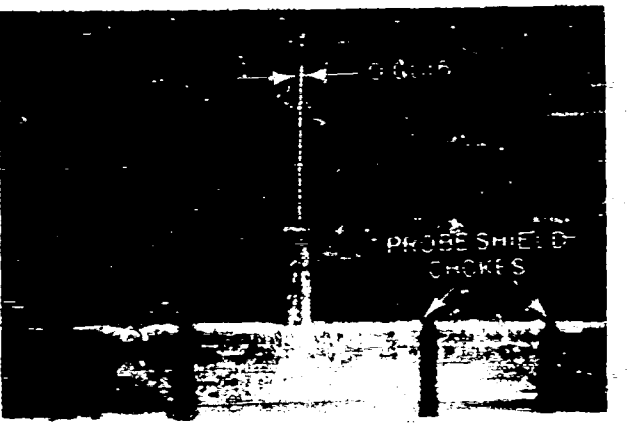

Fig. 5. Probe and probe holder emerging from probe carriage.

Crystal Detector

Commercial crystals (1N53's) proved to be too insensitive for use with the 50-kMc SWI; hence, a built-into-wave guide" type crystal was developed. A cross-sectional view (Fig. 6) and an exploded view (Fig. 7) show the general construction of the detector which is similar to designs used by other research groups.[4, 5] A silicon slab is mounted flush with the inside wall (broad face) of a rectangular guide. The post supporting the silicon is insulated for low frequencies while being a part of the high frequency by-pass capacitor. The small size of the silicon slab (20 mil dia., 10 mil thick) reduces ohmic losses and permits a small opening in the wave-guide wall. A pointed tungsten wire is

4) W.C. King and W. Gordy, Phys. Rev. 93, 407 (1954); J.A. Klein, J.H.N. Loubser, A.H. Nethercot, Jr., and C.H. Townes, Rev. Sci. Instr. 23, 78 (1952).

5) C.M. Johnson, D.M. Slager, and D.D. King, Rev. Sci. Instr. 25, 213 (1954).

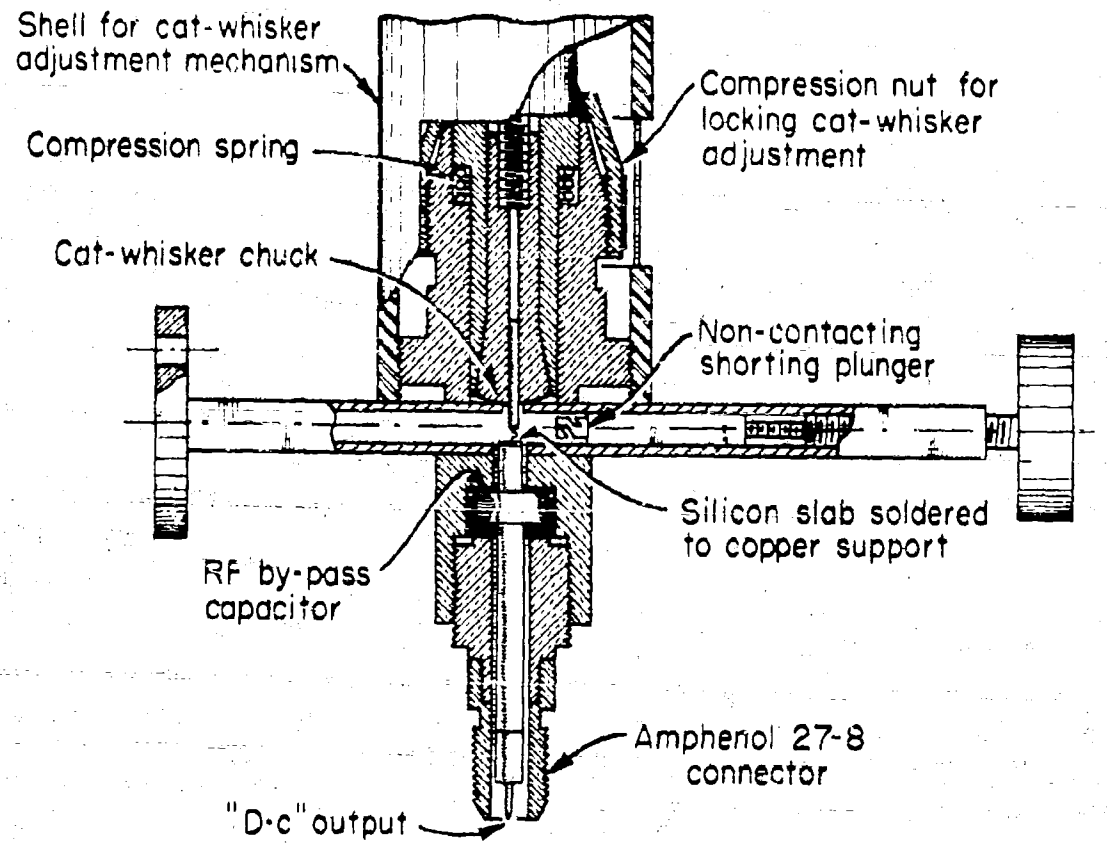

Fig. 6. Cross-sectional view of millimeter crystal detector.

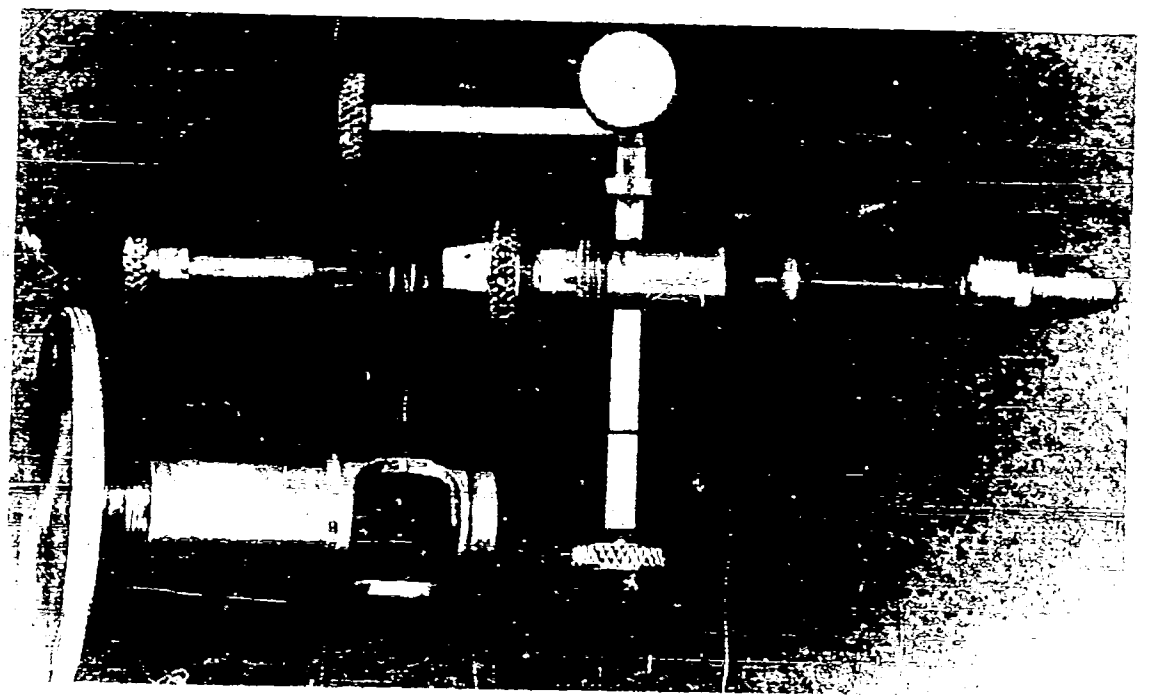

Fig. 7. Exploded view of 50-kMc crystal detector.

passed through the opposite wall of the guide and lowered to the surface of the silicon. Figure 8 shows a crystal with the "cat-whisker" in place. A differential screw mechanism permits adjustment of the "cat-whisker" to optimum pressure, while low-level 50-kMc energy is impressed on the crystal; in this way, the crystal is tuned for maximum output under typical operating conditions.

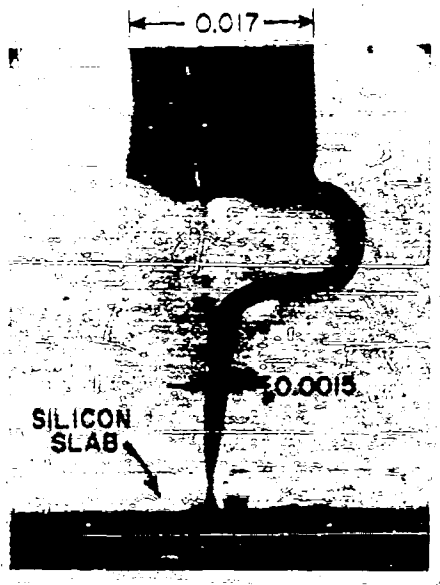

Fig. 8. Silicon, point-contact rectifier with cat-whisker in place.

The unique feature of the crystal mount is its versatility; both the "cat-whisker" and the silicon slab may be changed readily. Because the crystal holder has to be mounted off center on the probe carriage, it must be light in weight; hence the whisker adjustment mechanism was so designed that it could be removed after use.

The "cat-whiskers," like the probe, were made from gold plated, tungsten wire (1, 1.5, and 2 mils dia.). After shaping the wire in a simple jig, it was soldered into a silver tubing (17 mils o.d.). This tubing, in turn, is held in the crystal mount by a chuck (Figs. 6 and 7). The various steps in constructing a "cat-whisker" are shown in Fig. 9. After soldering, the gold plating on the straight portion of the tungsten wire was dissolved in concentrated hydrochloric acid (by applying a small d-c voltage). Finally, the wire was etched electrolytically to a point by a 10 M KOH solution. Variations in angle and sharpness of the point can be achieved at will by varying the voltage and length of exposure.

From the standpoint of maximum sensitivity of the crystal detector, the

most satisfactory points are extremely sharp: the radius of the end is ca. 1/30 that of the wire. This is somewhat sharper than the points used in commercial 1N53 crystals (Fig. 10).

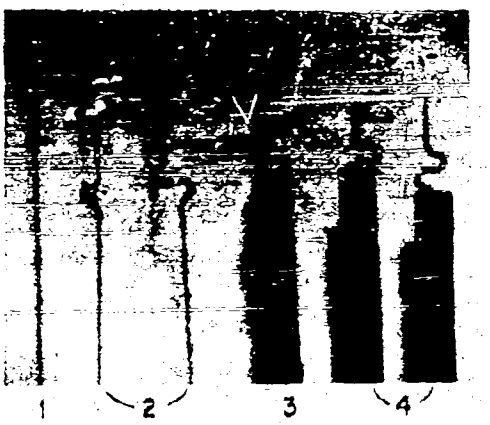

Fig. 9. Steps in constructing a cat-whisker: (1) tungsten wire is gold-plated; (2) then bent to desired shape using single or double bend; (3) the wire is soldered into a silver tube; and (4) etched to a sharp point.

Our silicon crystals with sharp pointed tungsten wire, properly adjusted, gave voltage outputs at least 10 times greater (power outputs 100 times greater) than the best 1N53's commercially available.[5, 6] Actual conversion figures were difficult to obtain because there are at present no accurate means of measuring the RF power incident on the crystal. For an input of approximately 3μw an output of 4.5 μμw was measured with our crystals, as compared to an output of 0.04 μμw for the 1N53 crystals. Burnout current and noise figure were not measured.

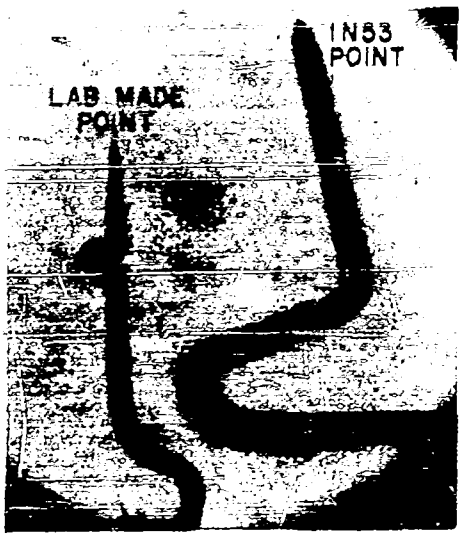

Fig. 10. Comparison of cat-whisker points.

The high-gain crystals are considerably less stable than the 1N53's. They are fragile, will not stand sudden shocks, and generally lose some of their sensitivity with time. However, in our use as detectors in the 50-kMc dielectrometer, these factors are not decisive.

---

6) J. M. Richardson and R. B. Riley, Nat. Bur. Standards (U.S.) Report 3580, March, 1956.

Sample holders

Samples placed directly in the wave guide block and backed by a short are difficult to remove. A more convenient method is to attach a shorted section of wave guide to the wave guide block, with the short containing a small center hole. Tight fitting samples can then be inserted into and removed from the detached sample holder. The length of a typical sample holder is a multiple of $\lambda_g/2$. This length places the joint between wave guide block and sample holder at a current maximum (for a sample-free guide) where the slightest fault in the joint would disturb the width of the "air nodes"* and thus be noticeable. A joint at a current minimum point of the air nodes would be less critical for measurements on the empty guide, hence faulty contact would not be easy to detect. However, with the insertion of a sample and the corresponding node shift, this faulty contact would introduce serious errors in the sample measurements.

Special holders for high or low temperature measurements have generally a longer electrical length (5 to 7 $\lambda_g/2$'s) in order to be able to heat or cool the sample while the SWI is kept near room temperature. A high-temperature holder is shown in Fig. 11. Above the heated section of the holder, a thermal resistance is introduced by thinning the wave guide wall. The indicator end of the holder is maintained at room temperature by a water jacket, while a reflecting shield above the holder prevents heat convection currents from reaching the SWI. Radiation losses are minimized by placing a metal shield around the heater insulation.

Because the amount of material required for a holder is small at these frequencies, it has become practical to build one from pure platinum. The holder is heated by a platinum ribbon and temperature measured by a Pt vs.

* "Air nodes" are nodes in the standing-wave pattern without a sample in the guide.

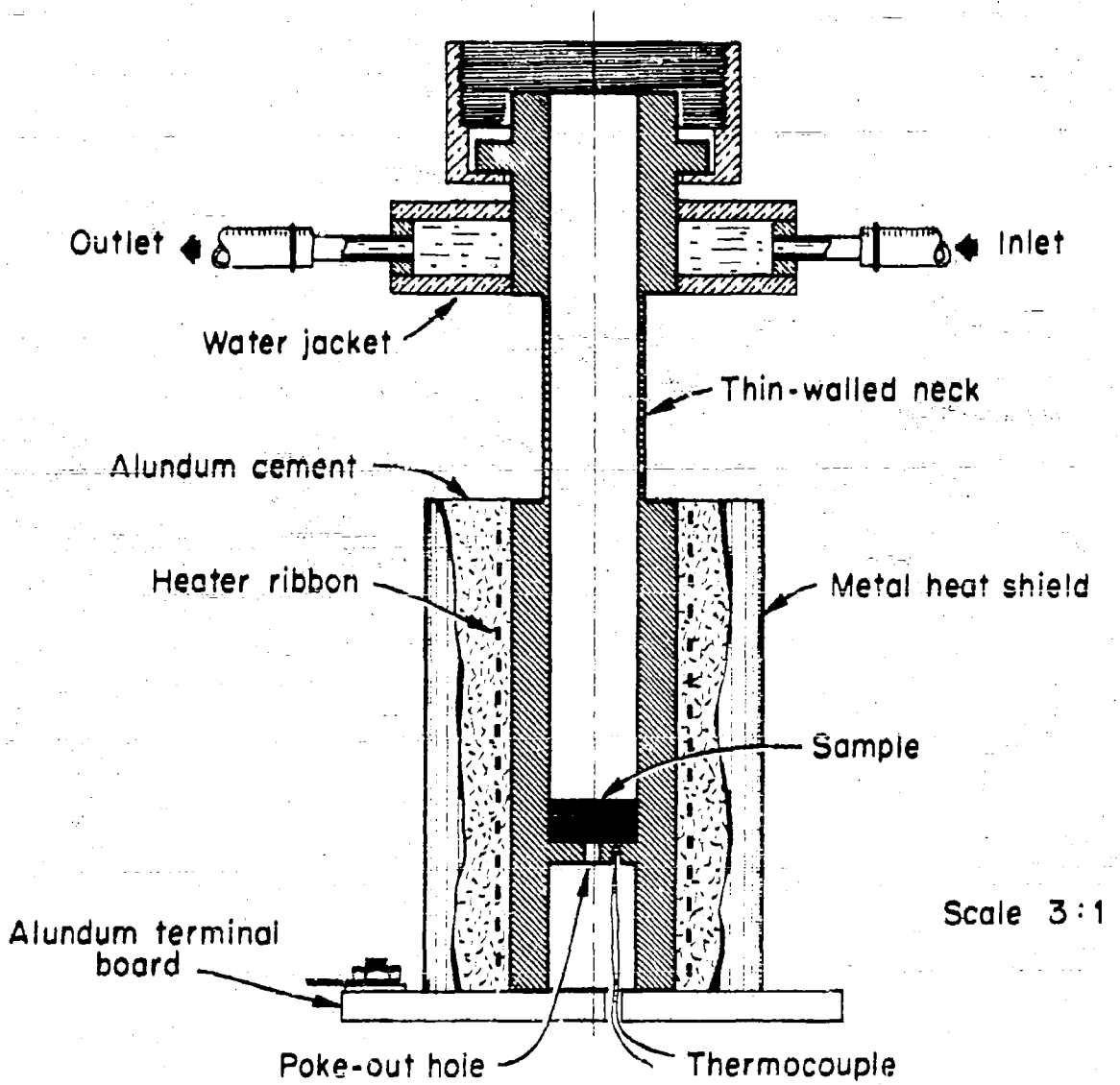

Fig. 11. High-temperature holder.

Pt-10% Rh thermocouple. This holder has been used up to 1200°C, and with minor changes in design should permit measurements as high as 1500°C.

Performance

Over 40 samples have been measured on the 50-kMc dielectrometer (Table 1). These measurements, with various tests, indicate the general performance limitations of the instrument. Relative dielectric constants ranging from 1 to 100 can be measured to 1 percent, and loss tangents to 5 percent or 0.0001, whichever is larger.

The most serious problem encountered was the appearance of higher-order modes in the circular guide. All measurements with the SWI take place at nodes in the main field pattern. Even the slightest amount of higher-order modes introduces errors in the readings. A circular guide is susceptible in particular to elliptical modes. In addition, a longitudinal slot of finite width in the guide upsets the current lines of the TE_{11} dominant mode and introduces a disturbance in the field pattern.

In spite of these difficulties the use of a circular guide is desirable for two reasons: circular samples can be made more easily and accurately than rectangular ones; and the sample cross-sectional area is greater in the circular guide, hence inaccuracies in sample fit are not as important.

A "matched" load test provides an indication of the mechanical quality of the SWI (Fig. 12). Ideally, if the probe would move longitudinally along the axis of the guide at a constant depth, the residual standing wave obtained by fixing the position of a load and moving the probe would be a sine wave, and a pattern very close to it is observed.

The longitudinal motion of the probe with respect to the slot can also be checked visually with the aid of a microscope. For this purpose, probe and probe holder are removed from the carriage, and the wave guide block and

Table 1. Dielectric constant and loss data for 50 kMc.*

Materials	κ'	tan δ x10^{-4}
Crystals		
Magnesium oxide	9.72	0.3
Lithium fluoride	8.73	2.6
Potassium bromide	4.79	2.2
Sodium chloride	5.83	4.8
Ceramics		
AlsiMag 243	5.72	10
AlsiMag 475	7.40	50
Bell Labs. F-66	6.25	12
Ceramic N750T96	83.0	54
Kearfott Alumina	9.3	0.1
Glasses		
Borosilicate glass	4.00	16.5
Corning 0010	5.72	137
0080	6.47	222
0090	7.66	127
0100	6.81	101
0120	6.52	112
1710	5.68	86
1990	8.19	63
1991	7.82	101
3320	4.63	85
7040	4.61	73
7050	4.74	88
7052	5.00	95
7070	3.95	15
7740	4.41	86
7900	3.77	13.8
8460	8.06	86
Phosphate glass 2043x	5.00	52
2279x	4.74	26
Fused quartz	3.75	2.0
Soda silicate glass (9% Na_2O, 91% SiO_2)	4.90	158
Soda silicate glass (12% Na_2O, 88% SiO_2)	5.08	178
Plastics		
Alathon 2	2.28	12
Bakelite BM-262	4.45	70
Bakelite BM-16981	4.50	56
Esso Paraffin 135°AMP	2.25	13
Glass laminate	3.79	89
Hysol 6000	2.92	101
Kel-F	2.25	48
Lucite	2.57	59
Nylon FM 10, 001	2.97	71
Paraplex P-43	2.84	96
Rexolite 1422	2.53	10.5
SE-450 (G.E.)	2.78	302
Stypol 16D	2.78	115
Teflon	1.97	3
Teflon laminate GB-112T	3.12	63

* The values given in this table are uncorrected for sample fit. As a result, the accuracy in κ' will vary from 1/2 to 2%.

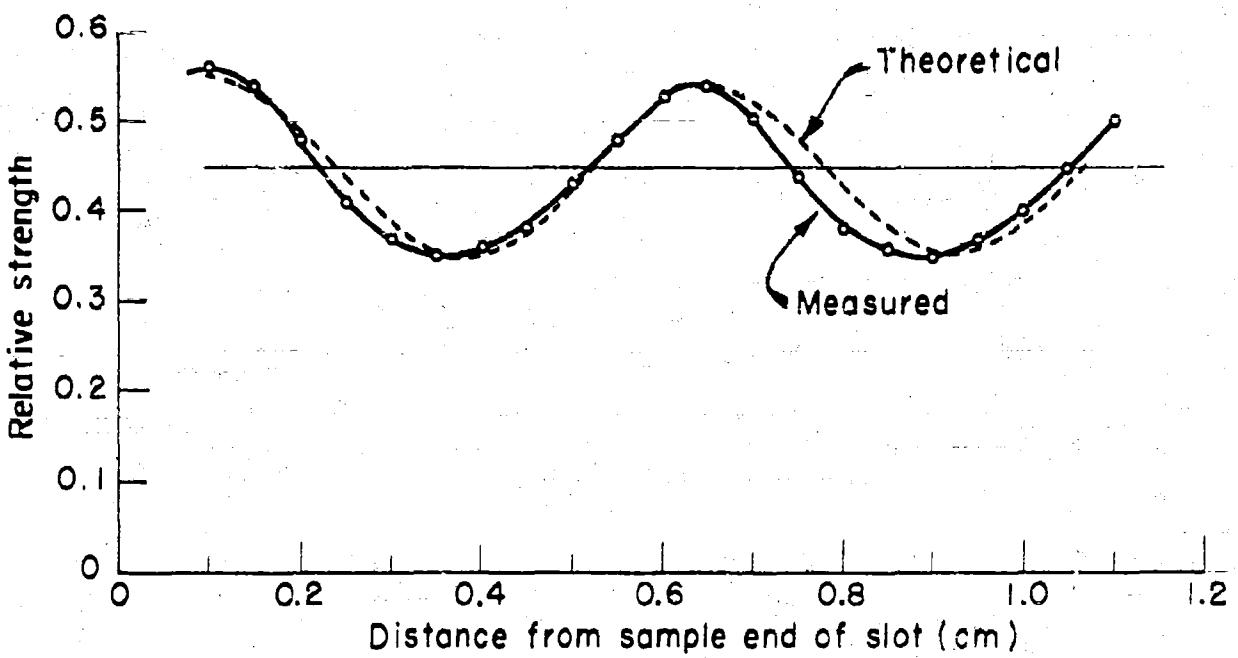

Fig. 12. "Matched" load test. Relative strength of standing-wave pattern for fixed load.

probe carriage are placed under a microscope with the interior of the guide illuminated. The slot can then be observed through the probe-holder hole in the carriage as it moves along its guide rods. The slot should at all times be located in the center of the probe-holder hole. The probe can be accurately centered with respect to the slot in this manner by trimming the V grooves. Such high accuracy in centering is required if slots as narrow as 4 mils are used with a 1-mil probe.

The most significant electrical test is a measurement of the air-node widths at several different nodes. Although the slot itself contains at most 3 nodes, the number of half wave lengths from the shorted end can be varied by using different sample holders. If a perfect short at the end of the guide and a perfect joint between holder and wave guide block exist, the air-node widths are given only by the wave guide wall losses. It follows that the widths

of consecutive nodes increase linearly with distance from the shorted end of the guide. A simple calculation of the theoretical node width (see Appendix) allows comparison with the actual values (Fig. 13). Day to day performance of the instrument can be checked by measuring the air nodes, and, in general, such measurements are a necessary and sufficient control.

Another yardstick of instrument performance and capability is its "sensitivity" and corresponding figure of merit. Generally speaking, the precision of the SWI is limited to the accuracy with which Δx_a, the node width of the empty guide, can be measured. The Laboratory for Insulation Research[7] has, for

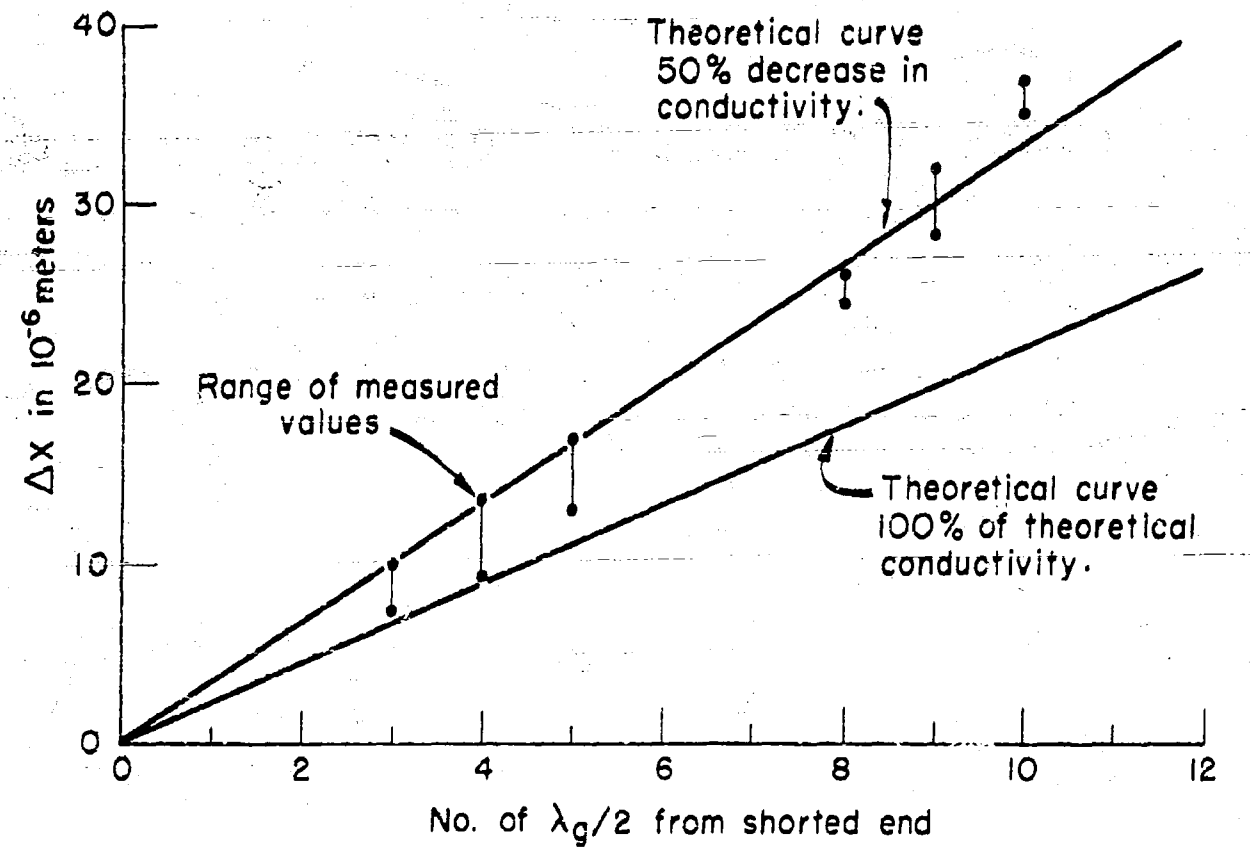

Fig. 13. Theoretical and actual air-node widths.

7) M.G. Haugen and W.B. Westphal, "The Design of Equipment for Measurement of Dielectric Constant and Loss with Standing Waves in Waveguides," N.D.R.C. Report XII, October, 1945, p. 5.

Table 2. Sensitivity of various standing-wave indicators. n is the number of half wave lengths between probe and end of empty line; m, the number of quarter wave lengths between probe and sample; a, the width of the rectangular guide; b, the height of the rectangular guide; tan δ_{wa}, the loss tangent produced by the wall loss in the empty guide; S_δ, the sensitivity; and V, the volume of sample.

Circular hollow guides							
Frequency Mcs	Diameter in.	tan δ_{wa}	S_δ n=2 m=3	S_δ n=4 m=5	% e for $S_\delta=10^{-5}$	Volume cm^2	$S_\delta xV$
9,500	0.870	.000069	.000515 e	-	1.94	2.21	.00114 e
24,000	0.360	.000099	.00069 e	-	1.45	0.147	.000101 e
50,000	0.172	.000157	.00110 e	-	0.97	0.017	.000019 e
50,000	0.172	.000157	-	.00043 e	2.38	0.085	.000036 e
Rectangular guides							
Frequency Mcs	a in.	b in.	tan δ_{wa}	S_δ n=2 m=3	% e for $S_\delta=10^{-5}$	Volume cm^2	$S_\delta xV$
9,500	0.900	0.400	.000047	.00028 e	3.57	1.26	.00035 e
24,000	0.420	0.170	.000062	.00035 e	2.86	0.096	.000034 e

comparison, defined the "sensitivity" of an SWI as the error in the calculated value of tan δ for a given error e in the measurement of the node width Δx_a. It depends not only on the performance of the instrument proper, expressed by e, but on the dielectric constant and loss of the sample, its length and position in the guide, and on the distance between probe and sample.

Table 2 gives the "sensitivity S_δ," the minimum detectable loss tangent, of the 50-kMc instrument for two sample thicknesses. For purposes of com-

parison, sensitivities are tabulated for SWI's used at 10 and 25 kMc.

The product of S_δ and V, the volume of the sample, is called "figure of merit" of the instrument. It readily indicates the instrument best suited for a particular size sample. The 50-kMc instrument has, for a particular sample thickness, a better figure of merit than any other instrument listed in Table 2.

Future Work

To develop a more sensitive and stable dielectrometer requires a more sensitive crystal detector; a superheterodyne pickup system; a frequency-stabilized oscillator; and modulation of the oscillator tube by external means, for example, by a ferrite switch or a mechanical chopper in the output guide.

Acknowledgements

The extension of the standing-wave method to 50-kMc was planned and supervised by W.B. Westphal to whom the author is greatly indebted. Acknowledgement is also extended to P. Kelleher, shop foreman, and E. Dufresne, machinist, who ably performed the highly skillful machine work required in constructing this instrument.

Finally, the author wishes to acknowledge the assitance in making the crystal detectors given by Sylvania Electric Company, Woburn, Mass.

APPENDIX

Calculation of Theoretical Attenuation

Textbooks on electromagnetic theory such as Ramo and Whinnery "Fields and Waves in Modern Radio" give the basic formula for attenuation in a circular guide as

$$\alpha = \frac{R_s}{a Z} \frac{1}{\sqrt{1 - \left(\frac{f_c}{f}\right)^2}} \left[\left(\frac{f_c}{f}\right)^2 + 0.42 \right] , \qquad (3)$$

where R_s is the surface resistivity, Z is the intrinsic impedance for free space, and a is the radius of wave guide. Let $(\lambda_g/\lambda_c)^2 = u$ and $1 + u = w$ and recall that $(f_c/f)^2 = (\lambda_o/\lambda_c)^2$ and $1/\lambda_o^2 = (1/\lambda_g^2) + (1/\lambda_c^2)$. Hence

$$\left(\frac{\lambda_c}{\lambda_o}\right)^2 = 1 + \left(\frac{\lambda_c}{\lambda_g}\right)^2 = 1 + \frac{1}{u} = \frac{w}{u} . \qquad (4)$$

Therefore $(f_c/f)^2 = u/w$; also $f = c/\lambda = c/\lambda_o$, where c is the velocity of light, λ_o, the free space wave length, λ_c, the cutoff wave length, and λ_g, the guide wave length. Also $\lambda_o^2 = (u/w)\lambda_c^2 = \lambda_g^2/w$ and thus

$$f^{1/2} = \frac{c^{1/2}}{\lambda_o^{1/2}} = \frac{c^{1/2}\, w^{1/4}}{\lambda_g^{1/2}} . \qquad (5)$$

By substituting Eqs. (4) and (5) into (3) with $R_s = 2.61 \times 10^{-7} f^{1/2}$ ohm for Cu; $Z = 377$ ohms; and $a = 0.218$ cm, we obtain

$$\alpha = \frac{2.61 \times 10^{-7}\, c^{1/2}\, w^{1/4}\, w^{1/2}}{(0.218)\,(377)\,\lambda_g^{1/2}} \left(\frac{u}{w} + 0.42\right) . \qquad (6)$$

If, in addition, we use the actual values: $\lambda_g = 1.05$ cm, $\lambda_c = 0.745$ cm, then $\alpha = 1.282 \times 10^{-3}$ nepers/cm.

This value of α can be used to determine a theoretical tan δ_w, the loss

tangent caused by wall losses. It can be shown[9] that $\tan\delta = \frac{2\alpha\beta}{(4\pi^2/\lambda_c^2) + \beta^2}$, where $\beta = 2\pi/\lambda_g$. Thus $\tan\delta_w = \frac{2(1.282\times10^{-3})(5.98)}{(4\pi/0.745)^2 + (5.98)^2} = 1.44\times10^{-4}$. A 50 percent decrease in conductivity, corresponding to a 22.4 percent increase in R_s, will increase $\tan\delta_w$ to 1.77×10^{-4}. Finally, for an air-filled guide,[8] $\Delta x = d_w \tan\delta_w$, where d = distance from node to end of guide, always a multiple of $\lambda_g/2$. For $d = \lambda_g/2$, $\Delta x/(\lambda_g/2) = \begin{cases} 2.19\times10^{-4} & \text{(for 100\% theoretical conductivity)} \\ 2.68\times10^{-4} & \text{(for 50\% theoretical conductivity)} \end{cases}$.

8) W.B. Westphal, "Techniques and Calculations Used in Dielectric Measurements on Shorted Lines," N.D.R.C. Report IX, 1945, pp. 12 and 32.